NFS Journal 38 (2025) 100213

Contents lists available at ScienceDirect

NFS Journal

journal homepage: www.elsevier.com/locate/nfs

Original article

Development of an *in vitro* triculture model of intestine inflammation to assess the immunomodulatory properties of cassava and roselle, two African green leafy vegetables

Nelly Fioroni [a,1,*], Maria Del Carmen Ponce de León Rodríguez [a,1], Nicolas Leconte [b], Claire Mouquet-Rivier [a], Caroline Guzman [a], Frédéric Boudard [a], Claudie Dhuique-Mayer [a,c], Myriam Collin [d], Anaïs Deglos [a], Emmanuelle Reboul [e], Ángela Bravo-Núñez [e], Caroline Laurent-Babot [a,*]

[a] UMR QualiSud, Université de Montpellier, Avignon Université, CIRAD, Institut Agro, IRD, Université de la Réunion, Montpellier, France
[b] UMR HSM, Université de Montpellier, CNRS, IRD, Montpellier, France
[c] CIRAD, UMR QualiSud, F-34398 Montpellier, France
[d] UMR DIADE, IRD/CIRAD F2F-Palmiers, Université de Montpellier, IRD, Montpellier, France
[e] Aix-Marseille Université, INRAE, INSERM, C2VN, Marseille, France

ARTICLE INFO

Keywords:
Caco-2/HT29 biculture
THP-1 macrophages
Leaf extract
In vitro digestion
Intestinal permeability
Cytokines

ABSTRACT

The intestine integrity and function are crucial for nutrient absorption and to prevent the entry of harmful antigens. In sub-Saharan Africa, frequent infections and enteric dysfunction can cause intestinal inflammation that is associated with stunting. Therefore, to study the anti-inflammatory effects of cassava and roselle leaves, commonly consumed as sauces, we developed an *in vitro* triculture model of intestine inflammation using intestinal Caco-2 (colorectal adenocarcinoma) and HT29-MTX (goblet cell-like) together with the macrophage-like THP-1 cells. Stimulation of this model with lipopolysaccharide/interferon-γ resulted in mucus over-production, higher pro-inflammatory cytokine release and loss of intestinal barrier integrity due to increased permeability. Polar/non-polar extracts and digested sauces from cassava and roselle leaves reduced cytokine production in both intestinal and THP-1 cells to different extents and restored barrier integrity and permeability. The developed and validated triculture model of inflamed intestine thus demonstrated the anti-inflammatory properties of cassava and roselle leaves, despite moderate responses.

1. Introduction

The primary function of the intestine is to absorb (micro)-nutrients, but it also regulates molecule entry and protects the body against antigens. Intestinal epithelial cells (IEC) and their apical junction complex form a semi-permeable barrier that limits translocation of luminal material to the lamina propria, where immune cells (*e.g.* macrophages, dendritic cells, lymphocytes) reside. The microbial community of the gastrointestinal tract is vital for maintaining intestinal homeostasis. In physiological conditions, the intestinal mucosa tolerates commensal microorganisms and food antigens through a finely regulated immunity mechanism. Imbalances can lead to inflammation, barrier defects, immune dysfunction, and nutrient malabsorption [1,2]. The aetiology of intestinal inflammation, the incidence of which is rising worldwide, remains unclear and involves multiple factors ([3]; [4]). Gut inflammation is linked to pathological conditions, such as enteric infections, diarrhoea, inflammatory bowel disease, metabolic syndrome, and non-communicable diseases (*e.g.* obesity and undernutrition) [5,6]. Stunting affects 22 % of children under five years old globally and 32 % in sub-Saharan Africa [7]. The environmental enteric dysfunction hypothesis suggests that chronic exposure to enteropathogens causes gut inflammation, contributing to stunted growth in these children [8,9]. Environmental enteric dysfunction is characterized by intestinal inflammation, villus atrophy, and crypt hyperplasia, leading to altered epithelial permeability and reduced intestinal absorptive capacity and ultimately in poor digestion and nutrient malabsorption [10,11].

* Corresponding authors.
E-mail addresses: nelly.fioroni@umontpellier.fr (N. Fioroni), caroline.babot@umontpellier.fr (C. Laurent-Babot).
[1] Nelly Fioroni and Maria del Carmen Ponce de León Rodríguez are co-first authors, they contributed equally to this work.

https://doi.org/10.1016/j.nfs.2025.100213
Received 7 October 2024; Received in revised form 13 January 2025; Accepted 13 January 2025
Available online 16 January 2025

Research on gut inflammation is crucial to understand the underlying mechanisms and find effective nutritional solutions, especially for low and middle-income countries. Improving the anti-inflammatory and antioxidant status by increasing the intake of fruits and vegetables rich in bioactive compounds can prevent malnutrition and the associated inflammation [12,13]. In sub-Saharan Africa, green leafy vegetables (GLVs) are widely consumed by the population and are key foods for their nutrition and dietary diversity [14]. Traditionally, GLVs are cooked as sauces to serve with cereal-based dishes. GLVs are excellent sources of iron, zinc, magnesium, potassium, and vitamin C, thus contributing to the daily requirements of these micronutrients, especially in children [15,16]. They are also rich in polyphenols (*e.g.* phenolic acids or flavonoids) and carotenoids (*e.g.* lutein, β-carotene), giving them strong antioxidant capacity [17]. Moreover, GLVs have demonstrated anti-inflammatory effects *in vitro* (murine and human immune cell models) [18,19] and *in vivo* using animal models (rats, mice, pigs) [20,21]. However, their impact on intestinal inflammation remains underexplored, particularly for cassava and African roselle leaves, which are widely consumed in Africa yet notably understudied.

In the past decades, *in vitro*, *ex vivo* and *in vivo* models have been developed to study intestinal epithelium functions, metabolism and inflammation. Animal models replicate organism-level physiology, but they raise ethical concerns and show species-specific responses, complicating their extrapolation to humans (Ponce de León Rodríguez, [22]). *In vitro* models reduce animal use and allow simpler and more reproducible studies of molecular mechanisms. The Caco-2 cell line (immortalized human colorectal adenocarcinoma cells) mimics enterocytes [23], but has limitations, including the absence of mucus layer [24]. To better replicate the human intestinal barrier, Caco-2 cells can be co-cultured with HT29-MTX cells, a stable clone derived from HT29 colorectal adenocarcinoma cells [25]. While not all HT29 cells produce mucus, those that differentiate into goblet cells like the HT29-MTX clone can produce a dense mucus layer due to the secretion of gel-forming mucins (MUC2, MUC5AC) [26,27]. Regarding inflammation, the Caco-2 cell line can produce some inflammatory molecules in response to cytokines or stimuli (*e.g.* lipopolysaccharides, LPS, from microorganisms), such as interleukin (IL)-1β, tumour necrosis factor (TNF)-α, interferon (IFN)-γ [28,29]. Several stimuli, such as IFN-γ and TNF-α, are known to act synergically on intestinal epithelial cells (F. [30,31]). However, for modelling intestinal inflammation, Caco-2 and HT29-MTX cells lack immune cells that are crucial for pro-inflammatory cytokine production [32]. Therefore, some groups tried to integrate immune cells, such as peripheral blood mononuclear cells or murine macrophage-like cells, in co-culture models [33,34]. As mixing human and murine cells in culture models is debated, the human THP-1 cell line, which can differentiate into macrophages, provides a solution [35,36] to better mimic physiological conditions. However, although this approach could be particularly useful in gut inflammation research, studies using co-culture of Caco-2, HT29-MTX, and THP-1 cells remain rare.

Based on literature, and particularly the works of [37–39,40] we developed an *in vitro* triculture model to evaluate the anti-inflammatory effects of food-derived bioactive compounds in the intestine. To mimic the intestinal barrier, we co-cultured Caco-2 cells with mucus-producing HT29-MTX cells grown on a filter and macrophage-like THP-1 cells at the basolateral side. The model was fully characterized (morphology, pro-inflammatory cytokine release, and barrier permeability changes) before using it to assess the anti-inflammatory effects of polar/non-polar extracts and of *in vitro* digested sauces of cassava and roselle leaves.

2. Materials and methods

2.1. Chemical and reagents

Dulbecco's Modified Eagle Medium GlutaMax™ (DMEM), RPMI 1640-GlutaMAX™ medium, nonessential amino acids, foetal bovine serum (FBS), penicillin–streptomycin (10,000 U–10 mg), trypsin-ethylenediamine tetraacetate (EDTA), Dulbecco's phosphate-buffered saline with or without calcium and magnesium (DPBS), IFN-γ, were purchased from Thermo Fisher Scientific (Saint-Quentin Fallavier, France). Phorbol 12-myristate 13-acetate (PMA), dexamethasone, LPS from *Escherichia coli* O55 B5, acid acetic, 4-(2-hydroxyethyl)-1-piperazineethanesulfonic acid (HEPES), Triton X-100, *Bacillus sp.* α-amylase (≥40.0 U/mg protein), porcine pepsin (≥2500 U/mg protein), porcine pancreatin (activity, 8 × USP specifications) and porcine bile extract were from Sigma Aldrich (Saint-Quentin Fallavier, France). Alcian blue and fast red were from Sigma-Aldrich (St. Louis, USA). Ethanol, hexane and sodium hydroxide (NaOH) were from HoneyWell Riedel-de Haën (Seelze, Germany).

2.2. Plant materials

2.2.1. GLV supply

The two African GLVs (one batch per species), cassava (*Manihot esculenta*) and roselle (*Hibiscus sabdariffa*), were purchased frozen from African grocery stores in Montpellier (France) in 2021. Leaves were then freeze dried, powdered, and stored at −20 °C.

2.2.2. Preparation of GLV polar and non-polar extracts

Solid-phase extraction, using the method reported by Fioroni et al. [17], was used to obtain polar (ethanol/water, 80/20) and non-polar (ethanol/hexane, 60/40) extracts from the freeze-dried GLVs. Extracts were stored at −20 °C until use.

2.2.3. Preparation of GLV-based model sauces

Freeze-dried GLVs were used to prepare simplified model sauces with dry matter content (12 %) and oil content (4 %) similar to those of field recipes based on Burkinabe and Beninese recipes [41]. Briefly, 5 g of powdered freeze-dried GLVs were mixed with 2.4 g peanut oil and 52 g water, then boiled for 5 min. After cooling, sauces were weighed, adjusted to 60 g with water, and stored at −20 °C until use.

2.3. Simulated GLV sauce digestion and micelle formation

A three-step *in vitro* digestion protocol, validated in human studies [42], was used after adaptations [43]. GLV model sauces (6 g) or peanut oil (control) were mixed with 16 mL 0.9 % NaCl and 1.25 mL salivary solution (pH 7) to mimic the oral phase. After 10 min at 37 °C, pH was adjusted to 4.00 ± 0.02 with 1 M HCl, and 1 mL porcine pepsin (P7012) (40 g/L in 0.1 M HCl) was added to mimic the gastric phase at 37 °C for 30 min. Then, the pH was adjusted to 6.00 ± 0.02 with 0.9 M sodium bicarbonate, followed by addition of 4.5 mL porcine pancreatin (P7545) solution (3 g/L in 0.1 M sodium citrate, pH 6) and 2 mL porcine bile (B8631) extract (127 g/L in 0.1 M sodium citrate, pH 6) to simulate the intestinal phase at 37 °C for 30 min.

Micellar fraction was separated from oil droplets and food particles by ultracentrifugation at 3000 rpm (Thermo Scientific SL 40 FR centrifuge in a TX-750 rotor), at 10 °C for 72 min, then filtered through 0.80 and 0.22 μm filters (Millipore, Burlington, MA, USA). The micellar fraction consists of micellar fractions containing non-polar compounds (including carotenoids) and a continuous polar phase that contains polyphenols. Aliquots of micellar fraction were diluted 1:5 with DMEM before assessing their anti-inflammatory effect.

2.4. Cell lines and culture conditions

The TC-7 subclone (ATCC: HTB-37) of the Caco-2 cell line [44] was generously provided by Monique Rousset (Nancy University, France). The HT29-MTX cell line (HT29-MTX 10–6) was obtained from the CelluloNet biobank BB-0033-00072 (UMS3444/US8/SFR Biosciences, Paris). Cells were maintained in 75 cm^2 flasks (Falcon™) at 37 °C and 5 % CO_2 in DMEM GlutaMax™ with 1 % nonessential amino acids, 10 %

heat-inactivated FBS, and 1 % penicillin-streptomycin (10 000 U–10 mg). At 80 % of confluence, cells were trypsinized with 0.05 % trypsin/1 mM EDTA. For experiments, Caco-2-TC7 cells were used between passages 56 and 65 and HT29-MTX cells between passages 22 and 67.

The human THP-1 cell line (monocytes; ATCC-TIB-202™) was maintained in suspension in RPMI 1640-GlutaMax™ medium with 10 % FBS and 1 % penicillin-streptomycin at 37 °C and 5 % CO_2. THP-1 cells were differentiated into macrophage-like cells by adding 20 ng/mL PMA for 48 h. After 24 h of rest in complete RPMI medium, cells were washed with DPBS (Ca^{+2}[+] Mg^{+2}[+]) containing 1 % FBS before use. THP-1 cells were used between passages 9 and 29.

2.5. Triculture model

Our first aim was to establish a stable Caco-2-TC7/HT29-MTX biculture system to mimic the human intestine with barrier integrity and mucus secretion. Caco-2-TC7 and HT29-MTX cells were plated alone or together (Caco-2-TC7/HT29-MTX biculture; 9:1 ratio) on 6-well ThinCert™ inserts (0.4 µm pore size, Greiner bio-one) at a density of 10^5 cells/cm^2 (day 1) and cultured in complete culture medium (changed every 2 days) for 15 days to allow their spontaneous differentiation into IEC. For the biculture, a 9:1 ratio was used to simulate the proportion of enterocytes and goblet cells in the intestine [45].

We then established a stable triculture of Caco-2-TC7/HT29-MTX cells with PMA-differentiated THP-1 cells to mimic the human intestine in a homeostatic state adapted from published protocols [37–39,40]. At day 12 of Caco-2-TC7/HT29-MTX biculture, THP-1 cells (2.6×10^4 cells/cm^2) were seeded in new 6-well plates (Greiner bio-one) and differentiated with 20 ng/mL PMA for 48 h, followed by washes with DPBS (Ca^{+2}[+] Mg^{+2}[+])/1 % FBS. Then, the Caco-2-TC7/HT29-MTX cell inserts were added to the wells containing the differentiated THP-1 cells (day 14) and grown in DMEM for 24 h (Fig. 1). Barrier integrity was assessed by measuring the transepithelial electrical resistance (TEER) and phenol red apparent permeability. Mucus secretion was assessed by histological staining and glycoprotein quantification.

The third objective was to induce an inflammation-like response in the stable triculture model. To this aim, at day 15, a pro-inflammatory cocktail of LPS-IFN-γ (1 µg/mL-50 ng/mL) was added to both compartments. These concentrations were chosen based on the literature and after preliminary adjustments. After 4 or 18 h of stimulation, the inflammatory markers including inducible nitric oxide synthase (iNOS) and cyclooxygenase-2 (COX-2), cytokines (TNF-α, IL-6, IL-8), and epithelial barrier integrity (TEER, apparent permeability) were measured. TNF-α release was measured after 4 h of stimulation, reflecting its early secretion during inflammation, while IL-6 and IL-8, secreted later, were measured after 18 h [35]. To confirm the protocol effectiveness, triculture were pre-incubated with 10 µM dexamethasone, a known anti-inflammatory compound, for 2 h before adding the pro-inflammatory cocktail.

2.6. GLV exposure effects

2.6.1. Effect of GLV extracts on cytokine production by LPS-stimulated THP-1 cells

THP-1 cells (5×10^4 cells/well) were seeded in 24-well plates in complete RPMI 1640-GlutaMAX™ medium with 20 ng/mL PMA and differentiated for 48 h, as described in Section 2.5. After 24 h, cells were incubated with GLV extracts (6.25–50 µg/mL) at 37 °C for 2 h. Then, cells were stimulated with LPS (100 ng/mL) and supernatants were collected at 4 and 18 h for cytokine (TNF-α, IL-6, and IL-8) measurements.

2.6.2. Effect of GLV extracts and digested sauces on the triculture model of intestine inflammation

The apical compartment of stable triculture was pre-incubated with GLV extracts (50 µg/mL) or micellar fractions (diluted 1:5 with DMEM) for 2 h before the addition of LPS-INF-γ (1 µg/mL-50 ng/mL) to induce inflammation. After 4 h or 18 h of incubation, cytokine production was measured in the apical and basolateral medium as well as epithelial barrier integrity and cytotoxicity.

2.7. Lactate dehydrogenase (LDH) assay to measure cytotoxicity

To test cell viability in the different experimental conditions, LDH

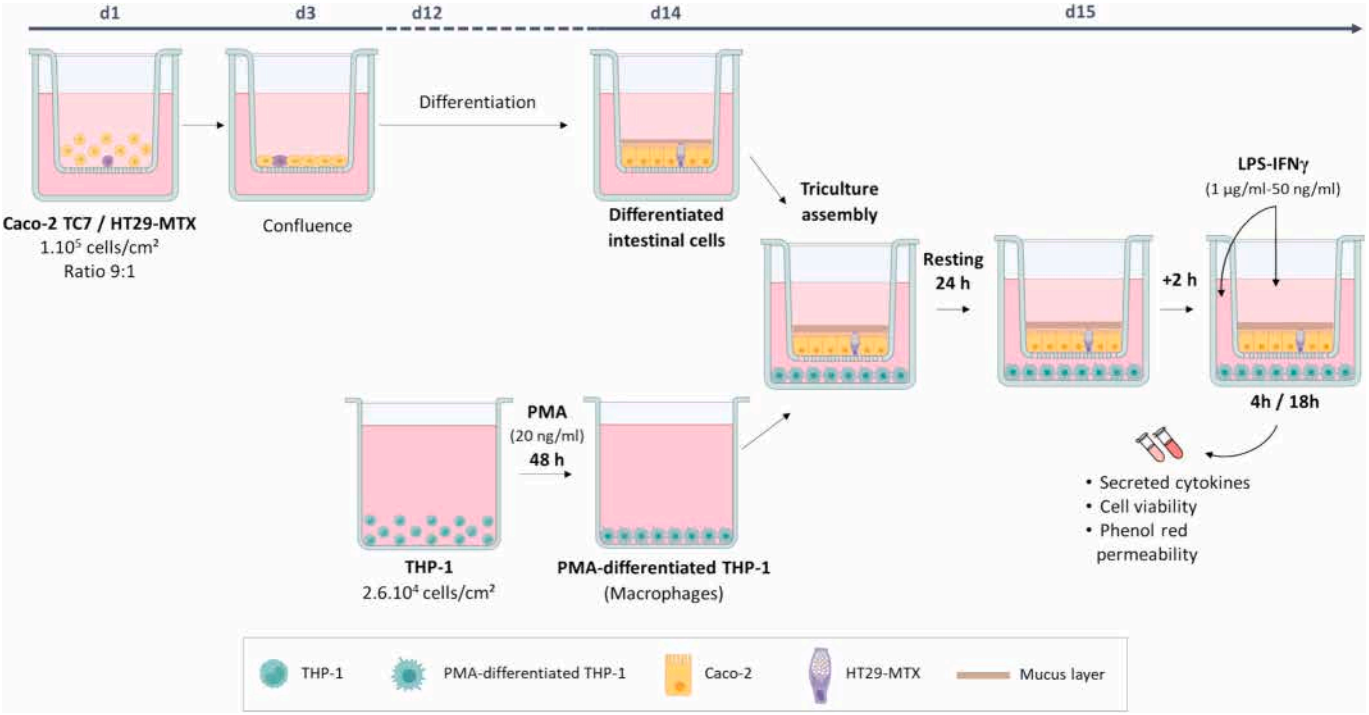

Fig. 1. Schematic representation of the *in vitro* triculture model protocol.

release into the apical medium was quantified by spectrophotometry using the LDH Activity Assay Kit (Sigma-Aldrich, Saint-Quentin Fallaviers, France) following the supplier's instructions.

2.8. Barrier integrity assessment

2.8.1. TEER measurement

The integrity of intestinal monolayers (single and biculture) was monitored daily by TEER measurement with the Millicell®-ERS Voltmeter until confluence and during medium changes (three times per week). In the triculture system, TEER was assessed before co-culture with THP-1 cells, after 24 h of rest, and after incubation with LPS/IFN-γ for 18 h. TEER values were expressed as Ohms (Ω).

2.8.2. Phenol red apparent permeability (Papp)

Phenol red apparent permeability (Papp) was measured as previously described [46]. After two washes with DPBS (Ca^{+2}[+] Mg^{+2}[+]), 1 mL of 1 mM phenol red in DPBS (Ca^{+2}[+] Mg^{+2}[+]) with 20 mM HEPES at pH 7.4 was added to the apical side and 1 mL of DPBS with 20 mM HEPES in the basolateral side. Following incubation at 37 °C for 1 h, phenol red concentration in the basolateral compartment was measured by reading the absorbance at 560 nm after the addition of 10 % NaOH (0.1 N). The trans-epithelial flux was expressed as Papp coefficient according to the following equation:

$$Papp = \frac{C}{C_0} \bullet \frac{V}{t} \bullet \frac{1}{A}$$

where C is the phenol red concentration after 60 min (mM), C_0 is the initial phenol red concentration (mM), t is the diffusion time (s), V is the basolateral compartment volume (mL), and A is the filter membrane area (cm^2).

2.9. Mucus staining with alcian blue in Caco-2-TC7/HT29-MTX cell biculture

In Caco-2-TC7 and HT29-MTX cell single cultures and in Caco-2-TC7/HT29-MTX cell biculture (9:1), mucus from HT29-MTX cells was stained with alcian blue and alkaline phosphatase from differentiated Caco-2 cells with fast red (SIGMAFAST™ Fast Red TR/Naphthol AS-MX Tablets, St. Louis, USA). Alcian blue was dissolved in 3 % acetic acid and added to the apical side at room temperature for 30 min. After washing with DPBS (Ca^{+2}[−] Mg^{+2}[−]), cells were stained with fast red at 37 °C. The reaction was stopped with water and samples were observed under an inverted optical microscope (Nikon Eclipse TE200, Minato, Tokyo, Japan).

2.10. Histological staining of mucus in Caco-2-TC7/HT29-MTX cell biculture

To observe mucus production by histochemestry in Caco-2-TC7/HT29-MTX cell biculture (9:1), at day 16, cells were gently rinsed with cold DPBS (Ca + 2[−] Mg + 2[−]) /4 % sucrose/3 % acetic to avoid mucus elimination. Cells were fixed with ice-cold methanol-Carnoy's fixative solution (60 % anhydrous methanol, 30 % chloroform, 10 % acetic acid) for 15 min. After fixation, cells were gently rinsed 3 times and rehydrated with ice-cold DPBS/4 % sucrose/3 % acetic. Culture inserts were removed and membrane were cut in small piece and embedded in DPBS/2.5 % degassed agarose, dehydrated through a graded series of ethanol, and embedded in cold-polymerizing resin Technovit 7100 methacrylate (Heraeus Kulzer GmbH, Wehrheim, Germany). Specimens were mounted on bloc/histobloc with Technovit resin 3040 (Heraeus Kulzer GmbH, Wehrheim, Germany). Samples were cut (4 µm of thickness) with a Microtome Microm HM355S (Thermo Scientific, Waltham, USA), placed on clean slides and dried. Tissue sections were stained with Mayer's Mucihematein Modified reagent, ready to use (Electron Microscopy Sciences, Hatfield, England) for 20 min at room temperature and briefly washed with tap water to remove excess dye. The slides were then washed three times in milliQ water bath, each for 5 min. After drying, staining intensity was evaluated microscopically and slides were mounted with Q Path® Isomount 2000 mounting medium (VWR international, Radnor, USA) and 0.15 mm coverslips.

2.11. Mucus quantification by glycoprotein measurement

The periodic acid/Schiff (PAS) stain was used to quantify mucin, the main mucus glycoprotein in cultures [47]. Cells were lysed with 200 µL 1 % Triton X-100 in DPBS and incubated with 0.5 % periodic acid at 37 °C for 2 h. Then, the Schiff reagent was added at room temperature for 30 min. Absorption was measured at 555 nm using a Spectro UV–Vis Infinite 200 Pro plate reader (Tecan Group Ltd., Grödig, Austria), with a calibration curve from 10 to 600 µg/mL using porcine mucin.

2.12. Quantification of cytokines and inflammation-related enzymes

2.12.1. Enzyme-Linked Immuno-Sorbent Assay (ELISA)

TNF-α, IL-6 and IL-8 were quantified using ELISA kits (Human TNF alpha Uncoated ELISA, Human IL-6 Uncoated ELISA, Human IL-8 Uncoated ELISA) according to the manufacturer's instructions (Invitrogen™ by Thermo Fisher Scientific, Vienna, Austria).

2.12.2. Reverse transcription quantitative polymerase chain reaction (RT-qPCR) analysis

For gene expression analysis by RT-qPCR, total RNA was extracted from harvested cells using the NucleoSpin® RNA/Protein kit (Macherey-Nagel, Hoerdt, France) and concentrated, if needed, using the NucleoSpin® RNA Clean-up Kit XS (Macherey-Nagel, Hoerdt, France). RNA purity was assessed by spectrometry (Thermo Scientific™ NanoDrop™ One/OneC, Waltham, USA) and for finer quantification, with a Qubit™ 4 fluorometer (Invitrogen™, Carlsbas, USA) and the Qubit™ RNA BR Assay kit (Invitrogen™, Carlsbas, USA). Then, cDNA was synthesized by RT with 1 µg of total RNA and the LunaScript®RT SuperMix kit (New England Biolabs Inc., Ipswich, USA) following the manufacturer's instructions. The RT-qPCR analyzes were carried out at the qPCR platform of the University of Montpellier, France, using the LightCycler® 480 System thermocycler in 384-well block (Roche, Penzberg, Germany) with 0.5 µL diluted cDNA (1/20) and 1 µL of master mix prepared with the SensiFAST ™ SYBR® No-ROX kit (Bioline Meridian Bioscience, Cincinnati, USA). The programme used was as follows: 5 min at 95 °C for enzyme activation, 45 cycles with denaturation at 95 °C for 10 s, 10 s pairing step at 64 °C, and 10 s elongation step at 72 °C. The primer sequences (Table 1) were selected with the NCBI Primer Blast application. The relative expression level for each gene was normalized to that of the housekeeping genes *RPLP0* and *RPL37A* for Caco-2 and HT29-MTX cells, and *RPLP0* and *ACTB* for THP-1 cells [48,49,50].

2.13. Immunofluorescence staining

Immunofluorescence staining was used to assess the expression of ZO-1, occludin, claudin (tight junction proteins) and of MUC5AC (mucin) in the biculture and triculture models. Cells were rinsed with ice-cold DPBS/4 % sucrose/3 % acetic acid, fixed with 4 % paraformaldehyde/4 % sucrose in DPBS for 20 min, and incubated with 0.1 % Triton X-100 for 3 min. Then, cells were incubated in Image-IT® Fx Signal Enhancer (Cell Signaling Technology, Danvers,USA) for 30 min and blocked with DPBS/Fish Gelatin Blocking Agent 1× solution (Biotium, Fremont, USA) for 60 min. Cells were incubated (4 °C overnight) in BlockAid™ Blocking Solution (Thermo Fisher Scientific, Waltham, USA) with the following primary antibodies against occludin (2 µg/mL) from Atlas antibodies, and ZO-1 (2.5 µg/mL), claudin (5 µg/mL) and MUC5AC (3 µg/mL) from Abcam. After washing with PBS-Fish Gelatin Blocking Agent 1×, cells were incubated with Alexa-conjugated

Table 1
Primer pairs used to quantify cytokine gene expression in intestinal and immune cells.

Genes	Primers sequences (5′→3′)	Concentration	PCR efficiency
NOS2	F-CCGAGGCAAACAGCACATTC R-CTGAGGGCTTTGCTGAGGTC	0.6 μM	1.95
COX2	F-GCTGTTCCCACCCATGTCAA R-TTCCGGTGTTGAGCAGTTTTCT	0.4 μM	2
TNF	F-TTCCCCAGGGACCTCTCTCT R-AGGGTTTGCTACAACATGGGC	0.4 μM	1.97
IL6	F-CCAGAGCTGTGCAGATGAGTACA R-GGCATTTGTGGTTGGGTCAGG	0.6 μM	1.97
IL8	F-AGACAGCAGAGCACACAAGC R-CACAGTGAGATGGTTCCTTCC	0.6 μM	2
IL10	F-GGCGCTGTCATCGATTTCTTC R-CACTCATGGCTTTGTAGATGCC	0.4 μM	1.96
RPLP0	F-TCTACAACCCTGAAGTGCTTGAT R-CAATCTGCAGACAGACACTGG	0.4 μM	2
RPL37A	F- TCTGTGGCAAAACCAAGATGAAGA R-TTACCGTGACAGCGGAAGTG	0.4 μM	1.93
ACTB	F-GATCATTGCTCCTCCTGAGC R-CCGGACTCGTCATACTCCTG	0.4 μM	1.87

secondary antibodies at 37 °C for 60 min; anti-rabbit Alexa Fluor 488 (4 μg/mL); and anti-mouse Alexa Fluor 633 (4 μg/mL) from Thermo Fisher Scientific (Saint-Quentin Fallavier, France). Cell nuclei were counterstained with DAPI (3 μg/mL in DPBS-sucrose) in the dark for 15 min (Euromedex, Souffelweyersheim, France). Samples were mounted on clean slides with Prologold™ Gold antifade reagent (Thermo Fisher Scientific, Waltham, USA) and 0.17 mm coverslips. Fluorescent images were captured with a 880 Multiphoton confocal microscope (Carl Zeiss Microscopy GmbH, Jena, Germany) using Zeiss ZEN software at the Confocal Microscopy Platform - MRI in Montpellier, France. The Imaris imaging software (Andor Technology, Belfast, Northern Ireland) was used to reconstruct 3D images from z-stack data.

2.14. Statistical analysis

All data were expressed as the mean ± standard deviation (SD). Data were analysed with Statgraphics Centurion 19.0 using one-way ANOVA followed by the Fisher's least significant difference (LSD) test. A p-value <0.05 was considered significant. When homogeneity of variance was not respected (Levene's test), a logarithmic nonparametric test (Games–Howell test) was used.

3. Results

3.1. Characterization of Caco-2-TC7/HT29-MTX cell biculture

3.1.1. Barrier integrity assessment

TEER values increased progressively in both Caco-2-TC7 cell single-culture and Caco-2-TC7/HT29-MTX cell biculture monolayers for 3 days after seeding (Fig. 2A). The highest TEER values (at confluence; day 3) were significantly lower in biculture (580 Ω.cm^2) than in Caco-2-TC7 cells alone (775 Ω.cm^2). Conversely, membrane permeability was similar in monocultures and biculture (data not shown).

3.1.1.1. Mucus secretion. After 16 days of culture, the apical side of Caco-2-TC7/HT29-MTX cell biculture was stained with alcian blue (acidic mucins secreted by HT29-MTX cells) and fast red (alkaline phosphatase, a marker of Caco-2 cell differentiation) (Fig. 2B). The staining patterns showed well-differentiated Caco-2-TC7 cells and a mucus layer produced by HT29-MTX cells. The presence of both red and blue staining in Caco-2-TC7/HT29-MTX cell biculture confirmed the growth and distribution of both cell types. Moreover, red multicellular "bump-like" areas, characteristics of Caco-2-TC7 cells, were interspersed with blue HT29-MTX cells. Quantification using PAS staining confirmed the enhanced mucus secretion in Caco-2-TC7/HT29-MTX cell biculture compared with Caco-2-TC7 cell monocultures (+49 %, $p < 0.05$) (Fig. 2C).

Lastly, staining with mucicarmine (mucins) (Fig. 2D) of Caco-2-TC7/HT29-MTX cell biculture at day 16 showed the presence of both cell types, of an apical portion distended by abundant mucus-laden granules in HT29-MTX cells, and of a thin mucus layer.

3.2. Optimization of the triculture model conditions

3.2.1. Characterization of stable triculture of Caco-2-TC7/HT29-MTX cells with PMA-differentiated THP-1 cells

To assess the impact of THP-1 cells on the Caco-2-TC7/HT29-MTX cell barrier integrity, TEER and Papp were monitored over 48 h. In triculture, TEER values slightly but significantly decreased after 24 h (−15 % compared with control biculture) (Fig. 3A). This indicated that differentiated THP-1 cells induced a weak barrier disruption that did not lead to Papp increase (Fig. 3B). LDH release quantification showed no significant increase in stable triculture, in both apical and basolateral compartments, compared with biculture (data not shown).

3.2.2. Characterization of triculture after incubation with the LPS/IFN-γ cocktail to induce inflammation

3.2.2.1. Barrier integrity assessment. Incubation with LPS/IFN-γ strongly and progressively decreased the TEER values in stable triculture compared with control biculture **(−25 %)** (Fig. 3A). This indicates that the barrier-disrupting effects of THP-1 cells was exacerbated by inflammation induction. As expected, inflammation induction increased Papp, indicating higher barrier permeability (Fig. 3B). Pretreatment with dexamethasone prevented LPS/IFN-γ effects on TEER and permeability. The similar LDH concentrations in both apical and basolateral compartments of triculture incubated or not with LPS/IFN-γ (with/without dexamethasone) indicated that LPS/IFN-γ and dexamethasone did not have any cytotoxic effect (data not shown).

3.2.2.2. Immunofluorescence staining of tight junctions. To determine whether the permeability increase induced by incubation with LPS/IFN-γ was linked to tight junction disruption, the expression of tight junction proteins (ZO-1, occludin, claudin) was assessed by immunofluorescence (Fig. 4A). In biculture, ZO-1, occluding and claudin were homogeneously and clearly expressed, defining the cell perimeter and enabling the apical membrane identification. In triculture incubated with LPS/IFN-γ, the distribution of tight junction proteins was altered: staining decreased in intensity and became irregular. The intracytoplasmic fluorescence signal increased, indicating a delocalization of tight junction proteins from the apical membranes and a rearrangement of their cellular organization. The specific analysis of ZO-1, an essential component of the tight junctional complex that is normally located toward the apical side of epithelial cells, showed that upon incubation with LPS/IFN-γ, in triculture, ZO-1 signal intensity decreased at the apical side and increased at the basolateral side with intracytoplasmic accumulation (Fig. 4B). This indicated ZO-1 expression delocalization and reorganization.

3.2.2.3. Mucus production. MUC5AC staining was increased in triculture incubated with LPS/IFN-γ compared with biculture (Fig. 4C), indicating higher mucus production by HT29-MTX cells in inflammatory conditions.

3.2.2.4. TNF-α, IL-6, and IL-8 production. Cytokine release (expressed as the percentage of the concentration in stable triculture) was measured in the apical and basolateral compartments of biculture, stable triculture, and triculture incubated with LPS/IFN-γ for 18 h (with/without

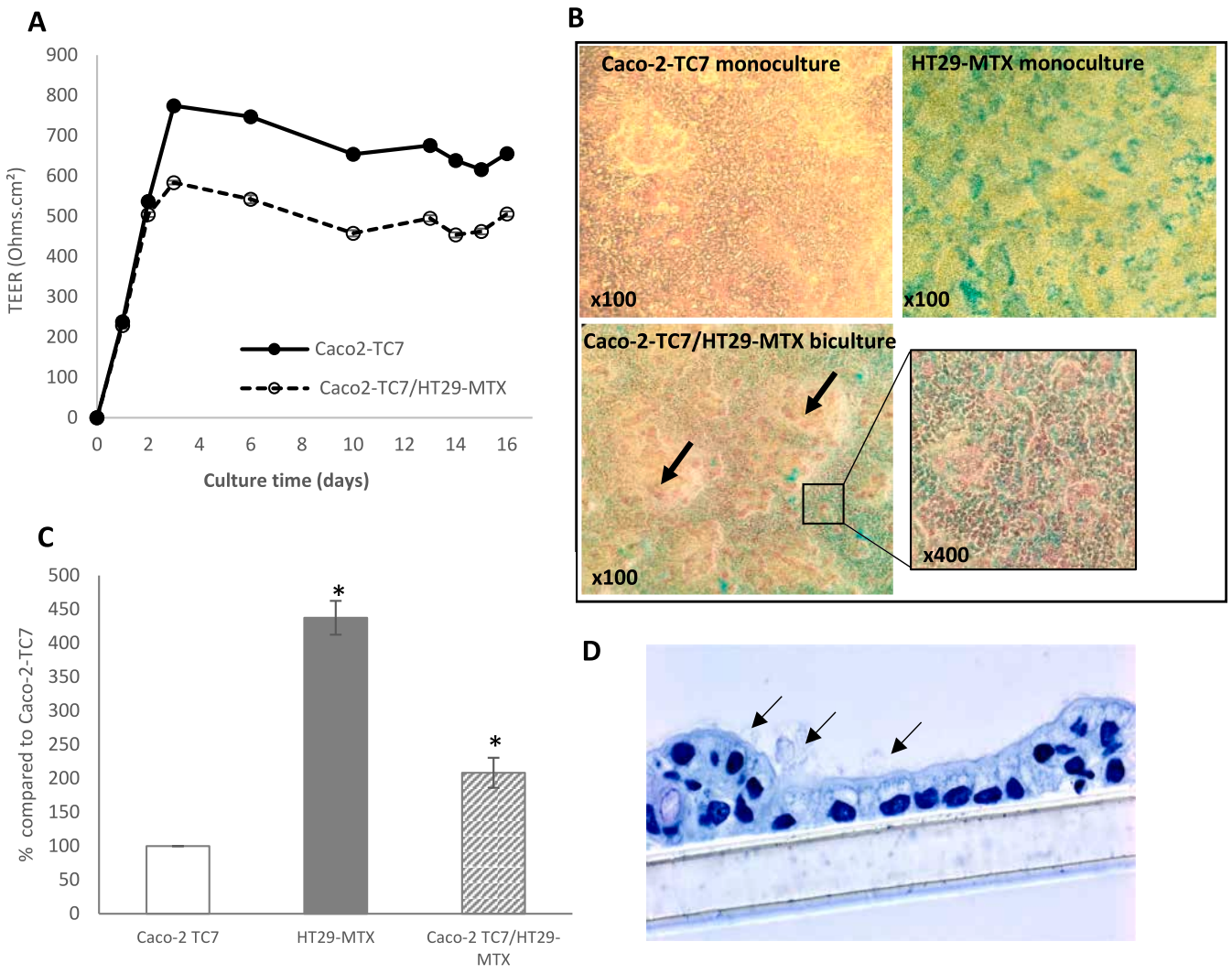

Fig. 2. Characterization of Caco-2-TC7/HT29-MTX cell biculture A. TEER values of Caco2-TC7 cells alone and bicultured with HT29-MTX cells at different time points expressed as ohms.cm^2. B. Caco2-TC7 cells (single culture) stained with fast red (left), HT29-MTX cells (single culture) stained with alcian blue (right), and Caco-2-TC7/HT29-MTX cell biculture (9:1 ratio) stained with fast red and alcian blue (bottom). Arrows show "bump-like" areas characteristic of Caco-2-TC7 cells. C. Mucin quantification by PAS stain in Caco2-TC7 and HT29-MTX single cultures and Caco-2-TC7/HT29-MTX cell biculture, expressed as percentage of positive-Caco-2-TC7 cells. *$p < 0.05$ *versus* Caco2-TC7 cells. D. Histological staining of biculture Caco-2-TC7/HT29-MTX with Mayer's Mucihematein. Arrows show mucus layer. TEER: transepithelial electrical resistance. (For interpretation of the references to colour in this figure legend, the reader is referred to the web version of this article.)

dexamethasone pretreatment) (Fig. 3C). In the apical medium, IL-6 and TNFα levels were very low (<15 pg/mL) in all culture models with no significant difference. Only IL-8 concentration significantly increased upon inflammation induction (1200 pg/mL) compared with stable triculture (280 pg/mL). This increase was prevented by pre-incubation with dexamethasone (300 pg/mL). In the basolateral compartment, the concentration of all three cytokines increased upon incubation with LPS/IFN-γ (values up to 15,000 pg/mL for TNFα, 300 pg/mL for IL-6, and 180,000 pg/mL for IL-8) compared with stable triculture. Dexamethasone prevented this inflammatory response.

3.2.2.5. Gene expression by RT-qPCR. The expression of genes encoding inflammation-related enzymes (COX-2 and NOS2) and cytokines (TNF-α, IL-6, and IL-8) was evaluated in both Caco-2-TC7/HT29-MTX biculture and in triculture (after incubation or not with LPS/IFN-γ for 18 h) (Fig. 5). In IEC (apical compartment), *NOS2* (iNOS) and *IL8* (IL-8) expression was upregulated after exposure to LPS/IFN-γ for 18 h, while *COX2* and *TNF* gene expression did not change. *IL6* expression was not detectable (data not shown). In THP-1 cells (basolateral compartment), gene expression of all cytokines as well as *COX2* was enhanced by LPS/IFN-γ exposure, but not *NOS2*.

3.3. Application: assessment of inflammation modulation by cassava and roselle leaves

3.3.1. Effect of the leaf extract concentration on cytokine production by THP-1 macrophages stimulated with LPS

The effects of four concentrations of GLV polar and non-polar extracts on cytokine production by LPS-stimulated THP-1 cells were tested to select the most appropriate concentration for further studies. First, 0.1 % ethanol (the vehicle used, corresponding to the maximum ethanol concentration in the GLV extract at 50 µg/mL) had no effect on cytokine production (data not shown). Incubation of THP-1 cells with polar and non-polar cassava extracts (6.25–50 µg/mL) induced a concentration-dependent inhibition of TNF-α compared with the positive control (LPS-stimulated THP-1 cells): 34 % and 21 % of decrease at 50 µg/mL, respectively (Fig. 6A). Roselle extracts also attenuated TNF-α production, particularly the non-polar extract (−35 % at 50 µg/mL). Both cassava and roselle extracts induced a concentration-dependent inhibition of IL-6 production compared with the positive control: 50 % and 60

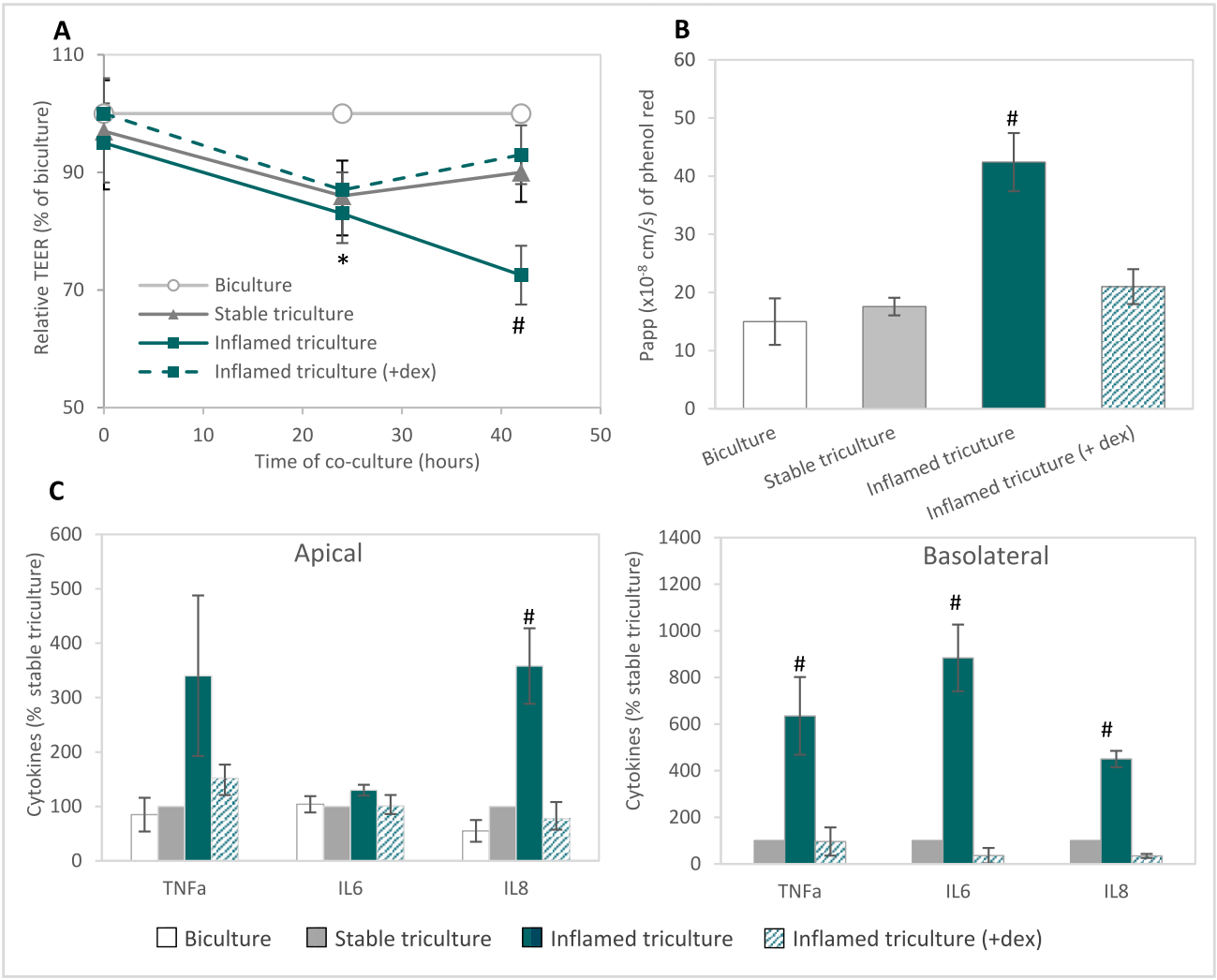

Fig. 3. Characterization of triculture of Caco-2-TC7/HT29-MTX cells with PMA-induced THP-1 cells. To induce inflammation, 24 h after the triculture set-up (stable triculture), cells were incubated with LPS-INF-γ (1 μg/mL-50 ng/mL) for 18 h (inflamed triculture). Dexamethasone (10 μM) was added as positive control (+dex) 2 h before the pro-inflammatory stimulation. **(A)** TEER (barrier integrity) measurement over 48 h after the triculture set-up, expressed as percentage of the biculture values. **(B)** Phenol red apparent permeability (Papp) at 48 h in triculture in which inflammation was induced or not. **(C)** TNF-α, IL-8 and IL-6 release in the apical and basolateral compartments in biculture, stable triculture and triculture in which inflammation was induced or not, expressed as percentage of the values in the stable triculture. Data are the mean ± SD (bars) ($n = 12$) from 4 experiments performed in triplicate. $^{*}p < 0.05$, stable triculture *versus* biculture. $^{\#}p < 0.05$, inflamed triculture *versus* stable triculture. TEER: transepithelial electrical resistance; TNF: tumour necrosis factor; IL: interleukin. (For interpretation of the references to colour in this figure legend, the reader is referred to the web version of this article.)

% decrease at 50 μg/mL for polar and non-polar extracts, respectively (Fig. 6B). Polar and non-polar cassava extracts also inhibited IL-8 production at 50 μg/mL by 40 % and 27 %. Conversely, only the non-polar roselle extract had an effect (33 % decrease) (Fig. 6C).

These experiments identified 50 μg/mL as the most effective concentration for inhibiting cytokine production by LPS-stimulated THP-1 cells. Moreover, LDH release was minimal at all tested extract concentrations and also with 0.1 % ethanol vehicle, confirming the absence of cytotoxic effects (data not shown).

3.3.2. Modulation of inflammation markers by GLV extracts and micellar fractions in the triculture model after inflammation induction by LPS/INF-γ

3.3.2.1. Barrier integrity assessment. In triculture stimulated with LPS/INF-γ, polar and non-polar cassava and roselle extracts maintained TEER values to levels comparable to those of stable triculture and even biculture (100–120 Ohm) (Fig. 7A and D). Polar cassava extracts (Fig. 7B) and both polar and non-polar roselle extracts (Fig. 7E) significantly limited the increase of barrier permeability observed upon incubation with LPS/INF-γ and also with ethanol. Similarly, cassava and roselle micellar fractions prevented the TEER decrease induced by LPS/INF-γ stimulation and maintained its values close to those observed in biculture (Fig. 7G). This was more pronounced with roselle micellar fractions, as confirmed by the permeability decrease (Fig. 7H). Thus, both polar and non-polar extracts and the digested sauces of cassava and roselle leaves protected the intestinal barrier integrity in inflammation conditions. Neither extracts nor micellar fractions caused cytotoxicity (evaluated by measuring LDH release) (data not shown).

3.3.2.2. TNF-α, IL-6, and IL-8 cytokine production. In the inflamed triculture, TNF-α, IL-6 and IL-8 production increased, compared with stable triculture. Analysis of the effects of vehicles (*i.e.* oil for micellar fractions and 0.1 % ethanol for extracts) on cytokine production showed that oil did not have any inhibitor effect, while 0.1 % ethanol exhibited some effects (described later). Neither cassava nor roselle extracts and micellar fractions decreased IL-6 production in triculture stimulated with LPS/INF-γ (data not shown).

In apical medium, only IL-8 could be quantified. Surprisingly,

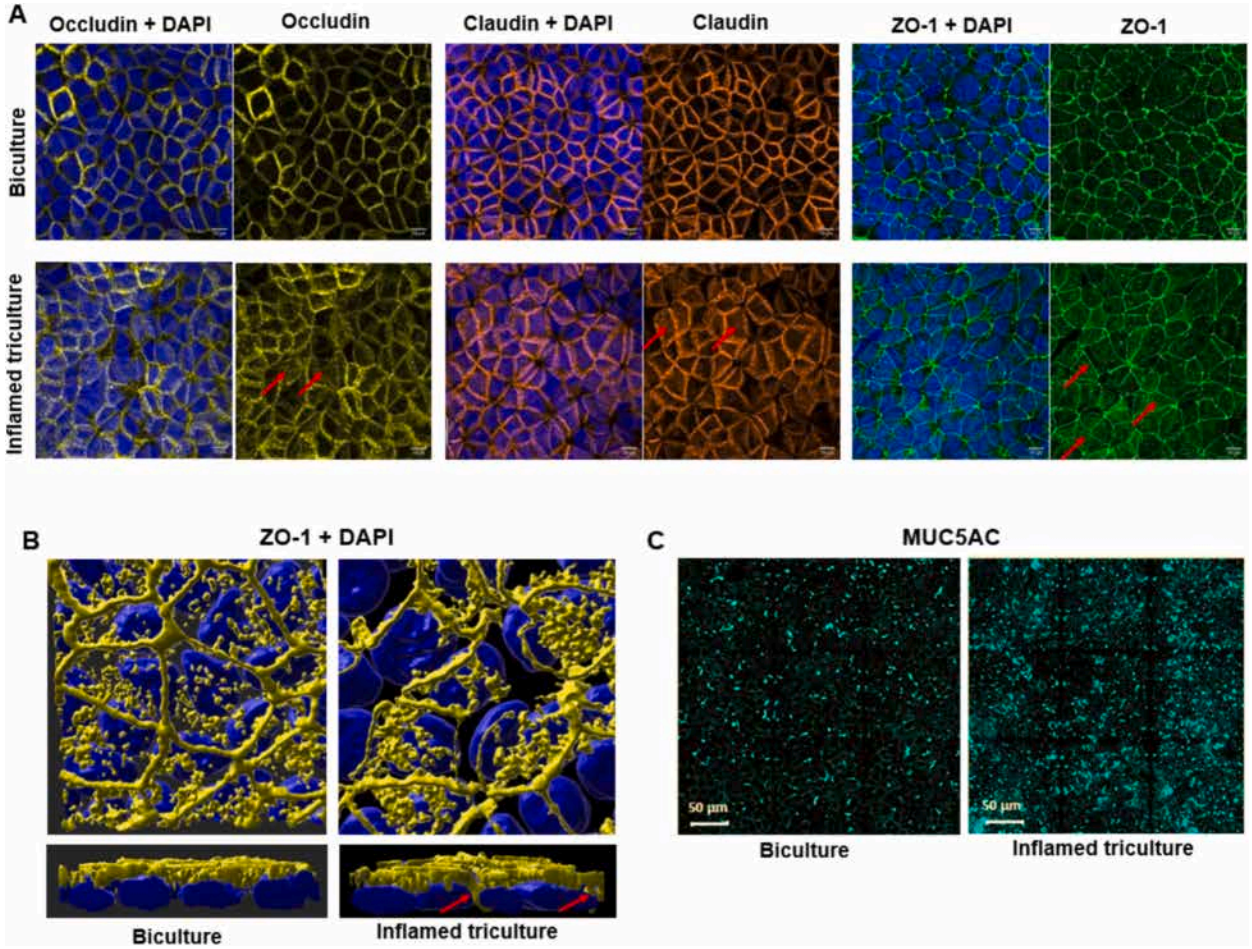

Fig. 4. Immunostaining of tight junction proteins (A,B) and MUC5AC (C) in Caco-2-TC7/HT29-MTX cell biculture and inflamed triculture of Caco-2-TC7/HT29-MTX cells with PMA-differentiated THP-1 cells (incubation with LPS-INF-γ, 1 µg/mL-50 ng/mL, for 18 h). (A) Images show occludin (yellow), claudin (orange) and ZO-1 (green) expression; cell nuclei are in blue. Arrows indicate the increased intracellular pool of tight junction proteins in inflamed triculture *versus* biculture. (B) 3D confocal laser scanning microscopy image of ZO-1 expression in a Caco-2-TC7/HT29-MTX cell biculture and in inflamed triculture. Images were reconstructed from z-stack files. Arrows show ZO-1 translocation from the apical to basolateral side. (C) MUC5AC staining in a Caco-2-TC7/HT29-MTX cell biculture and in a LPS-INF-γ-stimulated triculture. (For interpretation of the references to colour in this figure legend, the reader is referred to the web version of this article.)

ethanol decreased IL-8 secretion in triculture incubated with LPS/INF-γ (Fig. 7C). Compared with the 0.1 % ethanol control, non-polar cassava extracts showed a significant inhibition (Fig. 7C). Roselle polar and particularly non-polar extracts decreased IL-8 secretion by intestinal cells in LPS/INF-γ-stimulated triculture (Fig. 7F). Roselle micellar fractions also decreased IL-8 secretion by intestinal cells (−27 %), but not cassava micellar fractions (Fig. 7I).

In the basolateral medium, cassava extracts decreased the secretion of TNF-α and IL-8 by THP-1 cells compared with the 0.1 % ethanol control (Fig. 7C). Roselle extracts had no significant effect on TNF-α secretion, but the polar extract had a slight inhibitory effect on IL-8 (Fig. 7F). Cassava and roselle micellar fractions significantly and similarly decreased the secretion of TNF-α but not of IL-8 (Fig. 7I).

4. Discussion

In this study, we developed an *in vitro* intestinal model to assess the potential anti-inflammatory effects of bioactive compounds from foods. Given the context of high prevalence of malnutrition and environmental stress in sub-Saharan Africa, we focused on two African GLVs, cassava and roselle which are rich in micronutrients and bioactive compounds with antioxidant and anti-inflammatory properties [17].

Based on a literature review of *in vitro* models of intestine inflammation and their use (Ponce de León Rodríguez, [22]), we selected the most commonly used intestinal epithelial cell lines: Caco-2-TC7 cells with absorption capacity and mucus-secreting HT29-MTX cells (goblet cells) [51,25,24]. The Caco-2-TC7 clone could differentiate faster (15 days) than the parental line (30 days), while retaining the same characteristics and forming a more homogeneous and stable monolayer [52,44,53]. Mucus from HT29-MTX cells is crucial for estimating the intestinal permeability and absorption [27]. These cell lines are used in co-culture to closely mimic the *in vivo* intestinal physiology [54,26,55]. In our model, mucus production by HT29-MTX cells was demonstrated by alcian blue/fast red staining. Histological sections showed HT29-MTX cells among enterocytes, identifiable by their mucus pockets, and clusters of mucus on the apical membrane. Fluorescent labelling of MUC5AC, mucins produced by HT29-MTX cells [56], further confirmed the presence of the mucus layer.

Caco-2 cells can produce inflammatory mediators (*e.g.* cytokines or enzymes) in response to stimuli (LPS, IL-1β, TNF-α, IFN-γ) [28,29], but this response is often low. The presence of both epithelial and immune cells would better represent the physiological conditions than epithelial cells alone in an inflammatory context. The aim of our study was to establish a triculture model of Caco-2-TC7/HT29-MTX cells with human immune cells to mimic the human intestine in homeostatic conditions and upon inflammation. We selected the human monocyte-like THP-1 cell line because it can differentiate into macrophages and is widely used in inflammation models [35,36].

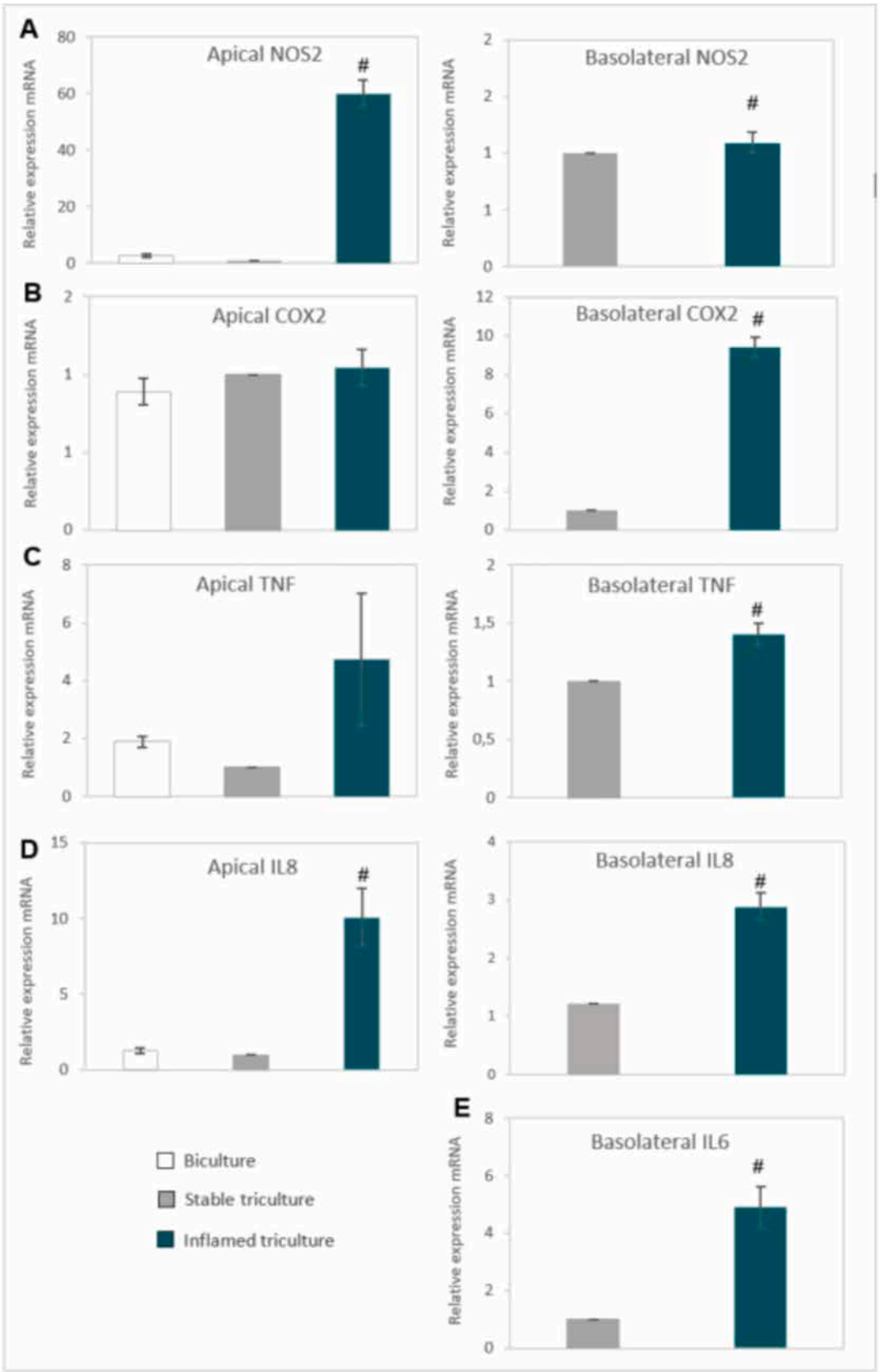

Fig. 5. Analysis by RT-PCR of the following genes: (A) *NOS2*, (B) *COX2*, (C) *TNF*, (D) *IL8*, and (E) *IL6* in cells from the apical and basolateral compartments in biculture, stable triculture and LPS-INF-γ-stimulated triculture (LPS-INF-γ, 1 μg/mL-50 ng/mL for 18 h). The relative expression level of each target gene was normalized to that of two housekeeping genes previously validated (*RPLP0* and *RPL37A* for biculture, RPLP0 and β-actin (ACTB) for THP-1) and compared to stable triculture. Data represent means ± SD (bars) ($n = 3$, triplicate measurements in one experiment). $^{\#}p < 0.05$, LPS-INF-γ-stimulated *versus* stable triculture. TNF, tumour necrosis factor; IL, interleukin.

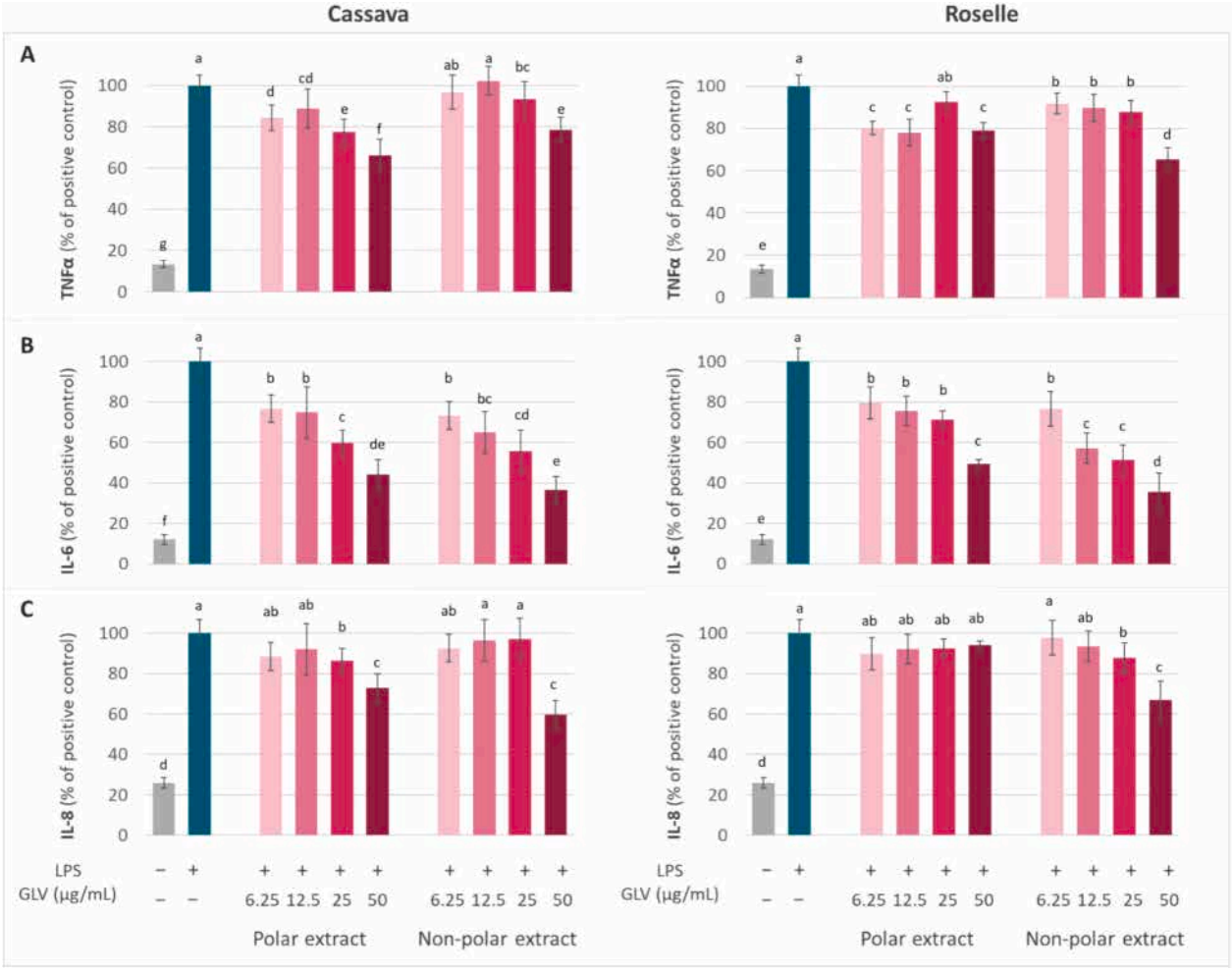

Fig. 6. Effect of different concentrations of polar and non-polar extracts of cassava and roselle leaves on TNF-α (**A**), IL-6 (**B**) and IL-8 (**C**) production by LPS-stimulated THP-1 macrophages. Cells were pre-incubated with GLV extracts (6.25, 12.5, 25, or 50 µg/mL) for 2 h before stimulation with LPS (100 ng/mL) for 4 h (TNF-α) or 18 h (IL-6 and IL-8). Data are the mean ± SD ($n = 6$) of two independent experiments performed in triplicate and expressed as the percentage of the positive control value (LPS). Differents letters indicate significant differences ($p < 0.05$).

To validate the model, we tested various parameters in normal and inflammatory conditions. TEER measurements indicated the establishment of barrier integrity (Caco-2-TC7/HT29-MTX biculture) through tight junction formation during the 14 days of differentiation, at a lower level than in monoculture, consistent with the literature [26], and probably due to differences in the rearrangement of the tight junction complex between cell types [57]. Addition of THP-1 cells slightly decreased TEER (−15 %), suggesting disruption of the cell monolayer integrity, likely *via* soluble factors, such as TNF-α [58,59]. The LPS-INF-γ cocktail strongly reduced TEER (−30 %), indicating increased membrane permeability during inflammation, confirmed by the higher phenol red transport. As shown in several studies, production of pro-inflammatory cytokines alters the tight junction complex, resulting in increased permeability [60,61]. In our model, TNF-α, IL-6, and IL-8 production and gene expression were strongly increased after pro-inflammatory stimulation, particularly in THP-1 cells, as expected and according to the literature [39,40]. Caco-2-TC7/HT29-MTX cell biculture showed limited TNF-α and IL-6 production, compared with other studies [62,63,64], highlighting the importance of including immune cells. The gene expression analysis showed *NOS2* upregulation in both Caco-2-TC7/HT29-MTX and THP-1 cells, and *COX2* upregulation only in THP-1 cells, likely due to the lower Caco-2 cell response to LPS [65]. This aligns with studies on intestinal inflammation, indicating that nitric oxide production is linked to colon lesions in inflammatory conditions [66–69]. COX-2, an oxidoreductase that produces prostanoids (prostaglandins and thromboxanes), is overexpressed during inflammation and is an inflammation marker.

Immunofluorescence microscopy revealed disruptions in the apical junction complex, with delocalization of claudin, occludin, and particularly ZO-1, which was translocated from the apical to the basolateral side, forming an undulating network, as previously reported [70,71]. This tight junction complex reorganization under inflammation conditions is consistent with previous studies [37,70,72]. Similarly, confocal fluorescence microscopy showed increased MUC5AC production upon stimulation, indicating heightened inflammation. This response supports mucus overproduction to trap bacteria, sustaining inflammation and to repair the damaged mucus layer [73,2]. Previous studies have also demonstrated a link between pro-inflammatory cytokines, such as TNF-α, IL-6 or LPS, and an increased production of MUC2 [74] and MUC5AC [75] both in HT-29 cells. Thus, upon incubation with LPS/IFN-γ, our triculture model exhibited an inflammation-like response, characterized by increased permeability, altered apical junction complex, mucus overproduction, and elevated pro-inflammatory cytokine and enzyme release [76,77,61]. Pre-incubation with dexamethasone confirmed the model responsiveness to anti-inflammatory agents, by partially restoring barrier integrity, permeability and reducing cytokine production.

Then, we investigated the anti-inflammatory effects of cassava and

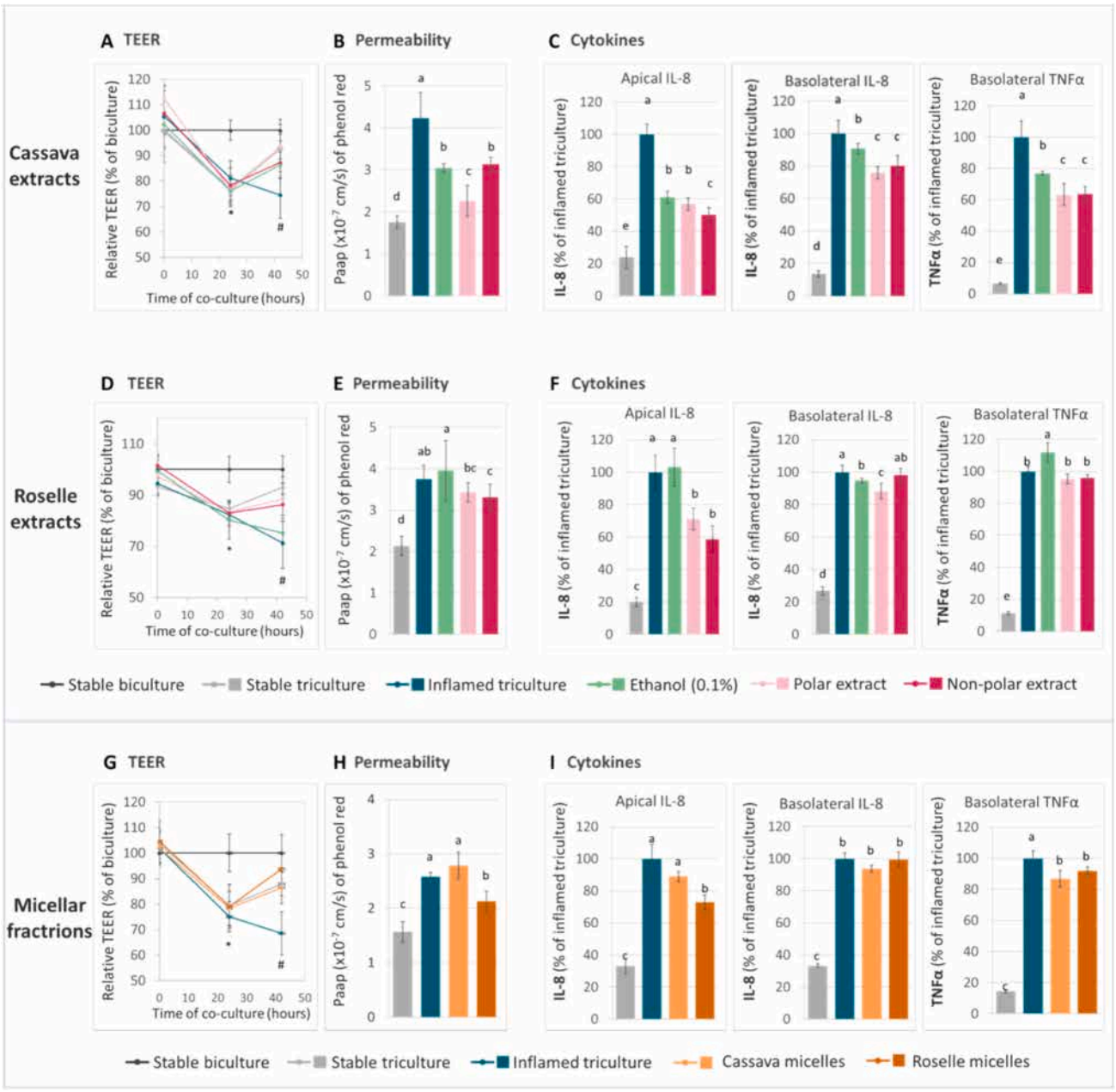

Fig. 7. Effect of polar and non-polar extracts of cassava (A-C) and roselle (D-F) on the production of various inflammation markers in the inflamed triculture model. Cells were pre-incubated with 50 μg/mL extracts for 2 h and stimulated with LPS-INF-γ (1 μg/mL-50 ng/mL) for 4 or 18 h. (A,D,G) TEER over 48 h after triculture set-up and expressed as percentage of the biculture values. (B,E,H) Phenol red apparent permeability (Papp). (C,F,J) Cytokine release in the apical or basolateral compartment after 4 h (TNF-α) or 18 h (IL-8) of stimulation, expressed as percentage of the values in the inflamed triculture. Data are the mean ± SD ($n = 3$) of triplicate measurements from one experiment. Different letters indicate significant differences ($p < 0.05$). #$p < 0.05$, stable triculture *versus* biculture. *$p < 0.05$, inflamed triculture (all conditions) *versus* stable triculture. TEER: transepithelial electrical resistance; TNF: tumour necrosis factor; IL: interleukin. (For interpretation of the references to colour in this figure legend, the reader is referred to the web version of this article.)

roselle leaves. Previous studies highlighted the *in vitro* antioxidant capacity of polar/non-polar extracts of these leaves due to the presence of bioactive compounds, such as carotenoids and flavonoids [17]. In LPS-stimulated THP-1 cells, polar/non-polar extracts of these GLVs inhibited TNF-α, IL-6 and IL-8 production by macrophages in a concentration-dependent manner, with the highest effect observed at 50 μg/mL, a concentration within plasma physiological levels. Cassava extracts showed stronger anti-inflammatory activity than roselle extracts, likely due to their twice higher flavonoid content (quercetin-3-*O*-rutinoside and kaempferol-3-*O*-rutinoside; 80 % of phenolic compounds). Previous studies showed flavonoid anti-inflammatory effects in LPS-induced murine macrophages (RAW 264.7) *via* the NF-κB and MAPK pathways [78,79]. Roselle effects may be partly explained by the presence of chlorogenic acid [17] that inhibits pro-inflammatory cytokines (IL-6, IL-1β, and TNF-α) in RAW 264.7 macrophages [80]. The both non-polar extract effects were likely due to lutein and β-carotene [17] that also inhibit the production of pro-inflammatory cytokines and enzymes (iNOS, COX-2) in murine macrophages following inflammation induction [81,82]. Our findings confirmed the anti-inflammatory effects of cassava and roselle leaves observed in previous studies in immune cells where they inhibit the production of pro-inflammatory cytokines and enzymes [83,20,84].

Overall, addition of polar/non-polar GLV extracts (50 μg/mL) to the apical side of the triculture model after incubation with LPS/IFN-γ

partially restored the cell monolayer integrity. This effect is likely due to their flavonoid and carotenoid contents that influence TEER and tight junction protein expression. For instance, quercetin and kaempferol (present in the polar extracts of cassava leaves) [17] enhance tight junction protein expression (claudin-4, ZO-2, occludin, claudin-1) and restore intestinal barrier function in Caco-2 cells [85,86]. Lutein (present in non-polar roselle extracts) reduces tissue damage and inflammatory factors and enhances tight junction protein expression (ZO-1, claudin-1, occludin) in dextran sulphate sodium-induced colitis in mice [87]. In an *ex vivo* mouse jejunum model, β-carotene, also present in non-polar roselle extracts, enhanced intestinal barrier function, as indicated by the increased TEER values [88].

Cytokine production modulation varied according to the GLV and cell type. In IEC (Caco-2-TC7/HT29-MTX biculture), only IL-8 was detectable and was decreased by polar/non-polar roselle extracts and non-polar cassava extracts. This suggests that roselle phenolic compounds and carotenoids could reduce IL-8 production in IEC, while only cassava carotenoids had an impact. Cytokine inhibition was less pronounced in THP-1 cells, with a slight inhibition of IL-8 and TNF-α by cassava extracts. This could be explained by the fact that the bioactive compounds must cross the IEC barrier to reach THP-1 cells. The effects on THP-1 cells may be mediated by polyphenols or their metabolites after absorption by enterocytes. Indeed, carotenoids require specific vehicles to be efficiently absorbed [89], which was not done in this study.

Isolated molecules provide initial insights, but they do not fully replicate the nutritional and physiological conditions due to the absence of the food matrix that determines the bioaccessibility and bioavailability after digestion. Therefore, we also evaluated the effects of cassava and roselle micellar fractions obtained after *in vitro* digestion of GLV sauces. Globally, micellar fractions showed weaker effects than extracts. Both micellar fractions restored TEER and barrier integrity after their alteration upon incubation with LPS/IFN-γ, but only roselle micellar fractions significantly reduced permeability. Roselle micellar fractions decreased IL-8 production by intestinal cells (apical side), and both micellar fractions modestly reduced TNF-α production by THP-1 cells with no effect on IL-8 (basolateral side). This suggests that the roselle bioactive compounds from digested sauce were more bioaccessible than those of cassava. Previous work in our laboratory showed that the bioaccessibility of roselle compounds [total polyphenols (58 %), β-carotene (2 %) and lutein (10 %)] was about two times higher than that of cassava compounds [total polyphenols (33 %), β-carotene (1 %) and lutein (4 %)]. Moreover, the modest inhibition of cytokine production by THP-1 cells could potentially be attributed to limited transport of micellar fractions, and thus bioactive compounds, across the IEC barrier. This could be explained by poor absorption of carotenoids due to low bioaccessibility, although other studies reported higher bioaccessibility rates for GLV carotenoids [90,42]. Alternatively, the low bioaccessibility of carotenoids observed in our study may be due to the low oil proportion in our sauces, chosen to increase dry matter and bioactive compound concentration. Nevertheless, according to the literature, carotenoid absorption by Caco-2 cells is generally low (~10 %) [91]. Besides, the low absorption of polyphenols can be explained by the need for hydrolysis by colonic microbiota before absorption. For instance, chlorogenic acid from roselle is absorbed as caffeic acid. Furthermore, rutin and the 3-*O*-rutinoside kaempferol present in cassava and roselle leaves are phenolic acids in esterified form and are less absorbed than in free form [92].

Overall, this study suggests a potential protective effect of cassava and particularly roselle sauces, after *in vitro* digestion, on intestinal barrier integrity and cytokine production related to intestinal inflammation. Although no study specifically examined these GLV effects on intestinal inflammation, many *in vitro* and *in vivo* works explored the role of polyphenols and carotenoids (also found in roselle and cassava leaves) on intestinal inflammation. For example, rutin has positive effects on intestinal inflammation in mice models, by reducing TNF-α, IL-1β, IL-6 or IFN-γ levels and increasing epithelial integrity [93,94]. β-carotene also improved the intestinal barrier function in a murine jejunum *ex vivo* model, by reversing villi shortening and lymphocyte infiltration and reducing IL-6 and TNF-α levels [88].

5. Conclusion

The *in vitro* cell triculture model developed in this study replicated the intestinal responses to inflammatory stimulation. As this model provides a straightforward and reproducible method for screening the preventive effects on gut inflammation of plant extracts and foods after *in vitro* digestion, it is a valuable tool for preliminary screening before *in vivo* validation. Both cassava and roselle extracts differently reduced inflammation markers (TNF-α and IL-8), likely due to differences in polyphenol and carotenoid contents and their mechanisms of action. Results obtained with digested GLV sauces also supported the anti-inflammatory effect of GLV consumption, likely due to their high bioactive compound contents. However, these findings require confirmation through further *in vivo* experiments using animal models to consider the whole digestive system including intestinal microbiota.

Funding

This research received no external funding.

Ethical statement

This work does not include experiments with humans or animals, and therefore does not require approval by an ethics committee.

CRediT authorship contribution statement

Nelly Fioroni: Writing – review & editing, Writing – original draft, Methodology, Formal analysis. **Maria Del Carmen Ponce de León Rodríguez:** Writing – original draft, Methodology, Formal analysis. **Nicolas Leconte:** Writing – original draft, Methodology, Formal analysis. **Claire Mouquet-Rivier:** Writing – review & editing, Supervision, Conceptualization. **Caroline Guzman:** Methodology. **Frédéric Boudard:** Methodology, Formal analysis. **Claudie Dhuique-Mayer:** Methodology, Formal analysis. **Myriam Collin:** Methodology. **Anaïs Deglos:** Methodology. **Emmanuelle Reboul:** Methodology, Formal analysis. **Ángela Bravo-Núñez:** Methodology. **Caroline Laurent-Babot:** Writing – review & editing, Writing – original draft, Methodology, Formal analysis, Conceptualization.

Declaration of competing interest

The authors declare that they have no known competing financial interests or personal relationships that could have appeared to influence the work reported in this paper.

Acknowledgements

We thank Philippe Clair from the qPCR platform/Montpellier GenomiX for useful advice.

References

[1] N. Di Tommaso, A. Gasbarrini, F.R. Ponziani, Intestinal barrier in human health and disease, Int. J. Environ. Res. Public Health 18 (23) (2021), https://doi.org/10.3390/ijerph182312836. Article 23.

[2] S.M. Vindigni, T.L. Zisman, D.L. Suskind, C.J. Damman, The intestinal microbiome, barrier function, and immune system in inflammatory bowel disease : a tripartite pathophysiological circuit with implications for new therapeutic directions, Ther. Adv. Gastroenterol. 9 (4) (2016) 606–625, https://doi.org/10.1177/1756283X16644242.

[3] A. Ali, N.T. Iqbal, K. Sadiq, Environmental enteropathy, Curr. Opin. Gastroenterol. 32 (1) (2016) 12–17, https://doi.org/10.1097/MOG.0000000000000226.

[4] R. Wang, Z. Li, S. Liu, D. Zhang, Global, regional and national burden of inflammatory bowel disease in 204 countries and territories from 1990 to 2019 : a systematic analysis based on the global burden of disease study 2019, BMJ Open 13 (3) (2023) e065186, https://doi.org/10.1136/bmjopen-2022-065186.

[5] I.G. Lempesis, V.E. Georgakopoulou, Physiopathological mechanisms related to inflammation in obesity and type 2 diabetes mellitus, World J. Exp. Med. 13 (3) (2023) 7–16, https://doi.org/10.5493/wjem.v13.i3.7.

[6] F. Stumpf, B. Keller, C. Gressies, P. Schuetz, Inflammation and nutrition : friend or foe? Nutrients 15 (5) (2023) 1159, https://doi.org/10.3390/nu15051159.

[7] UNICEF, Levels and trends in child malnutrition : UNICEF, in: World health Organization, Fund (UNICEF), United Nations Children's, World Bank, 2021. https://apps.who.int/iris/handle/10665/341135.

[8] S. Budge, A.H. Parker, P.T. Hutchings, C. Garbutt, Environmental enteric dysfunction and child stunting, Nutr. Rev. 77 (4) (2019) 240–253, https://doi.org/10.1093/nutrit/nuy068.

[9] F. Fontaine, S. Turjeman, K. Callens, O. Koren, The intersection of undernutrition, microbiome, and child development in the first years of life, Nat. Commun. 14 (1) (2023) 3554, https://doi.org/10.1038/s41467-023-39285-9.

[10] R. Crane, K.D. Jones, J. Berkley, La dysfonction entérique environnementale, 2014. https://docplayer.fr/26974262-La-dysfonction-enterique-environnementale-aperçu.html.

[11] H. Sies, C. Berndt, D.P. Jones, Oxidative stress, Annu. Rev. Biochem. 86 (2017) 715–748, https://doi.org/10.1146/annurev-biochem-061516-045037.

[12] M.H. Carlsen, B.L. Halvorsen, K. Holte, S.K. Bøhn, S. Dragland, L. Sampson, C. Willey, H. Senoo, Y. Umezono, C. Sanada, I. Barikmo, N. Berhe, W.C. Willett, K. M. Phillips, D.R. Jacobs, R. Blomhoff, The total antioxidant content of more than 3100 foods, beverages, spices, herbs and supplements used worldwide, Nutr. J. 9 (2010) 3, https://doi.org/10.1186/1475-2891-9-3.

[13] N. Pellegrini, M. Serafini, B. Colombi, D. Del Rio, S. Salvatore, M. Bianchi, F. Brighenti, Total antioxidant capacity of plant foods, beverages and oils consumed in Italy assessed by three different in vitro assays, J. Nutr. 133 (9) (2003), https://doi.org/10.1093/jn/133.9.2812. Article 9.

[14] R.-Y. Yang, G. Keding, African Indigenous Vegetables in Urban Agriculture (C. M. Shackleton, M. W. Pasquini, & A. W. Drescher, Éds.), Earthscan, 2009.

[15] A. Dehayem-Kamadjeu, J. Okonda, X-ray fluorescence analysis of selected micronutrients in ten African indigenous leafy vegetables cultivated in Nairobi, Kenya, Pan Afr. Med. J. 33 (296) (2019), https://doi.org/10.11604/pamj.2019.33.296.19501. Article 296.

[16] N.P. Uusiku, A. Oelofse, K.G. Duodu, M.J. Bester, M. Faber, Nutritional value of leafy vegetables of sub-Saharan Africa and their potential contribution to human health : a review, J. Food Compos. Anal. 23 (6) (2010) 499–509, https://doi.org/10.1016/j.jfca.2010.05.002.

[17] N. Fioroni, C. Mouquet-Rivier, E. Meudec, V. Cheynier, F. Boudard, Y. Hemery, C. Laurent-Babot, Antioxidant capacity of polar and non-polar extracts of four African green leafy vegetables and correlation with polyphenol and carotenoid contents, Antioxidants 12 (9) (2023), https://doi.org/10.3390/antiox12091726. Article 9.

[18] H.R. Tufts, C.S. Harris, Z.N. Bukania, T. Johns, Antioxidant and anti-inflammatory activities of Kenyan leafy green vegetables, wild fruits, and medicinal plants with potential relevance for kwashiorkor, Evid. Based Complement. Alternat. Med. (2015), https://doi.org/10.1155/2015/807158, 807158.

[19] Y.-Y. Yan, Y.-W. Wang, S.-L. Chen, S.-R. Zhuang, C.-K. Wang, Anti-inflammatory effects of phenolic crude extracts from five fractions of *Corchorus Olitorius* L, Food Chem. 138 (2–3) (2013), https://doi.org/10.1016/j.foodchem.2012.10.052. Article 2-3.

[20] H. Me, E.S. As, E.-A. Hi, M. Sm, E.-F. Am, Immunomodulatory and anti-inflammatory activities of the defatted alcoholic extract and mucilage of *Hibiscus sabdariffa* L. leaves, and their chemical characterization, J. Pharmacogn. Phytochem. 8 (4) (2019) 982–990.

[21] D. Orieke, O.C. Ohaeri, I.I. Ijeh, S.N. Ijioma, Gastrointestinal and uterine smooth muscles relaxant and anti-inflammatory effects of *corchorus olitorius* leaf extract in laboratory animal models, J. Ethnopharmacol. 247 (2020) 112224, https://doi.org/10.1016/j.jep.2019.112224.

[22] M.C. del Ponce De León Rodríguez, Développement d'un modèle in vitro d'inflammation intestinale par l'utilisation de lignées cellulaires humaines en co-culture pour l'étude des interactionsavec les micro-constituants alimentaires, 2019 [These de doctorat, Montpellier], https://www.theses.fr/2019MONTG009.

[23] Fogh, J., & Trempe, G. (1975). New human tumor cell lines. In J. Fogh (Éd.), Human Tumor Cells In Vitro (p. 115–159). Springer US. doi: https://doi.org/10.1007/978-1-4757-1647-4_5.

[24] H. Sun, E.C. Chow, S. Liu, Y. Du, K.S. Pang, The Caco-2 cell monolayer : usefulness and limitations, Expert Opin. Drug Metab. Toxicol. 4 (4) (2008) 395–411, https://doi.org/10.1517/17425255.4.4.395.

[25] T. Lesuffleur, A. Barbat, E. Dussaulx, A. Zweibaum, Growth adaptation to methotrexate of HT-29 human colon carcinoma cells is associated with their ability to differentiate into columnar absorptive and mucus-secreting cells, Cancer Res. 50 (19) (1990) 6334–6343.

[26] A. Béduneau, C. Tempesta, S. Fimbel, Y. Pellequer, V. Jannin, F. Demarne, A. Lamprecht, A tunable Caco-2/HT29-MTX co-culture model mimicking variable permeabilities of the human intestine obtained by an original seeding procedure, Eur. J. Pharm. Biopharm. 87 (2) (2014) 290–298, https://doi.org/10.1016/j.ejpb.2014.03.017.

[27] G.J. Mahler, M.L. Shuler, R.P. Glahn, Characterization of Caco-2 and HT29-MTX cocultures in an in vitro digestion/cell culture model used to predict iron bioavailability, J. Nutr. Biochem. 20 (7) (2009) 494–502, https://doi.org/10.1016/j.jnutbio.2008.05.006.

[28] S. Gong, J. Zheng, J. Zhang, Y. Wang, Z. Xie, Y. Wang, J. Han, Taxifolin ameliorates lipopolysaccharide-induced intestinal epithelial barrier dysfunction via attenuating NF-kappa B/MLCK pathway in a Caco-2 cell monolayer model, Food Res. Int. (Ottawa, Ont.) 158 (2022) 111502, https://doi.org/10.1016/j.foodres.2022.111502.

[29] H. Zhang, Y.I. Hassan, J. Renaud, R. Liu, C. Yang, Y. Sun, R. Tsao, Bioaccessibility, bioavailability, and anti-inflammatory effects of anthocyanins from purple root vegetables using mono- and co-culture cell models, Mol. Nutr. Food Res. 61 (10) (2017), https://doi.org/10.1002/mnfr.201600928.

[30] F. Wang, W.V. Graham, Y. Wang, E.D. Witkowski, B.T. Schwarz, J.R. Turner, Interferon-gamma and tumor necrosis factor-alpha synergize to induce intestinal epithelial barrier dysfunction by up-regulating myosin light chain kinase expression, Am. J. Pathol. 166 (2) (2005) 409–419, https://doi.org/10.1016/s0002-9440(10)62264-x.

[31] F. Wang, B.T. Schwarz, W.V. Graham, Y. Wang, L. Su, D.R. Clayburgh, C. Abraham, J.R. Turner, IFN-gamma-induced TNFR2 expression is required for TNF-dependent intestinal epithelial barrier dysfunction, Gastroenterology 131 (4) (2006) 1153–1163, https://doi.org/10.1053/j.gastro.2006.08.022.

[32] M.F. Neurath, Cytokines in inflammatory bowel disease, Nat. Rev. Immunol. 14 (5) (2014), https://doi.org/10.1038/nri3661 article 5.

[33] F. Guo, R. Tsao, C. Li, X. Wang, H. Zhang, L. Jiang, Y. Sun, H. Xiong, Polyphenol content of green pea (*Pisum sativum* L.) Hull under In vitro digestion and effects of digestive products on anti-inflammatory activity and intestinal barrier in the Caco-2/Raw264.7 Coculture model, J. Agric. Food Chem. 70 (11) (2022) 3477–3488, https://doi.org/10.1021/acs.jafc.2c00102.

[34] K.-M. Kim, Y.-S. Kim, J.Y. Lim, S.J. Min, H.-C. Ko, S.-J. Kim, Y. Kim, Intestinal anti-inflammatory activity of Sasa quelpaertensis leaf extract by suppressing lipopolysaccharide-stimulated inflammatory mediators in intestinal epithelial Caco-2 cells co-cultured with RAW 264.7 macrophage cells, Nutr. Res. Pract. 9 (1) (2015) 3–10, https://doi.org/10.4162/nrp.2015.9.1.3.

[35] W. Chanput, J. Mes, R.A.M. Vreeburg, H.F.J. Savelkoul, H.J. Wichers, Transcription profiles of LPS-stimulated THP-1 monocytes and macrophages : a tool to study inflammation modulating effects of food-derived compounds, Food Funct. 1 (3) (2010) 254–261, https://doi.org/10.1039/c0fo00113a.

[36] W. Chanput, J.J. Mes, H.J. Wichers, THP-1 cell line : An in vitro cell model for immune modulation approach, Int. Immunopharmacol. 23 (1) (2014) 37–45, https://doi.org/10.1016/j.intimp.2014.08.002.

[37] A.A.M. Kämpfer, P. Urbán, S. Gioria, N. Kanase, V. Stone, A. Kinsner-Ovaskainen, Development of an in vitro co-culture model to mimic the human intestine in healthy and diseased state, Toxicol. in Vitro Int. J. Published Assoc. BIBRA 45 (Pt 1) (2017) 31–43, https://doi.org/10.1016/j.tiv.2017.08.011.

[38] A.A.M. Kämpfer, M. Busch, V. Büttner, G. Bredeck, B. Stahlmecke, B. Hellack, I. Masson, A. Sofranko, C. Albrecht, R.P.F. Schins, Model complexity as determining factor for In vitro Nanosafety studies : effects of silver and titanium dioxide nanomaterials in intestinal models, Small 17 (15) (2021) 2004223, https://doi.org/10.1002/smll.202004223.

[39] A. Kaulmann, S. Legay, Y.-J. Schneider, L. Hoffmann, T. Bohn, Inflammation related responses of intestinal cells to plum and cabbage digesta with differential carotenoid and polyphenol profiles following simulated gastrointestinal digestion, Mol. Nutr. Food Res. 60 (5) (2016) 992–1005, https://doi.org/10.1002/mnfr.201500947.

[40] D. Marescotti, G. Lo Sasso, D. Guerrera, K. Renggli, P.A. Ruiz Castro, R. Piault, V. Jaquet, F. Moine, K. Luettich, S. Frentzel, M.C. Peitsch, J. Hoeng, Development of an advanced multicellular intestinal model for assessing immunomodulatory properties of anti-inflammatory compounds, Front. Pharmacol. 12 (2021), https://doi.org/10.3389/fphar.2021.639716.

[41] V. Greffeuille, C. Mouquet-Rivier, C. Icard Vernière, O. Laurencia, D. Hounhouigan, W. Amoussa Hounkpatin, P. Kayodé, F. Hama-Ba, Traditional Recipes of Millet, sorghum, and Maize-Based Dishes and Related Sauces Frequently Consumed by Young Children in Burkina Faso and Benin, 2010.

[42] E. Reboul, M. Richelle, E. Perrot, C. Desmoulins-Malezet, V. Pirisi, P. Borel, Bioaccessibility of carotenoids and vitamin E from their Main dietary sources, J. Agric. Food Chem. 54 (23) (2006) 8749–8755, https://doi.org/10.1021/jf061818s.

[43] A. Malapert, V. Tomao, M. Margier, M. Nowicki, B. Gleize, O. Dangles, E. Reboul, β-Cyclodextrin does not Alter the bioaccessibility and the uptake by Caco-2 cells of olive by-product phenolic compounds, Nutrients 10 (11) (2018) 1653, https://doi.org/10.3390/nu10111653.

[44] I. Chantret, A. Rodolosse, A. Barbat, E. Dussaulx, E. Brot-Laroche, A. Zweibaum, M. Rousset, Differential expression of sucrase-isomaltase in clones isolated from early and late passages of the cell line Caco-2 : Evidence for glucose-dependent negative regulation, J. Cell Sci. 107 (Pt 1) (1994) 213–225, https://doi.org/10.1242/jcs.107.1.213.

[45] I. Lema, J.R. Araújo, N. Rolhion, S. Demignot, Jejunum : the understudied meeting place of dietary lipids and the microbiota, Biochimie 178 (2020) 124–136, https://doi.org/10.1016/j.biochi.2020.09.007.

[46] S. Ferruzza, M.L. Scarino, L. Gambling, F. Natella, Y. Sambuy, Biphasic effect of iron on human intestinal Caco-2 cells : early effect on tight junction permeability with delayed onset of oxidative cytotoxic damage, Cell. Mol. Biol. (Noisy-le-Grand) 49 (1) (2003) 89–99.

[47] M. Mantle, A. Allen, A colorimetric assay for glycoproteins based on the periodic acid/Schiff stain, Biochem. Soc. Trans. 6 (3) (1978) 607–609, https://doi.org/10.1042/bst0060607.

[48] M. Krzystek-Korpacka, B. Szczęśniak-Sięga, I. Szczuka, P. Fortuna, M. Zawadzki, A. Kubiak, M. Mierzchała-Pasierb, M.G. Fleszar, Ł. Lewandowski, P. Serek, N. Jamrozik, K. Neubauer, J. Wiśniewski, R. Kempiński, W. Witkiewicz, I. Bednarz-

Misa, L-arginine/nitric oxide pathway is altered in colorectal Cancer and can be modulated by novel derivatives from Oxicam class of non-steroidal anti-inflammatory drugs, Cancers 12 (9) (2020), https://doi.org/10.3390/cancers12092594. Article 9.
[49] M.B. Maeß, B. Wittig, A. Cignarella, S. Lorkowski, Reduced PMA enhances the responsiveness of transfected THP-1 macrophages to polarizing stimuli, J. Immunol. Methods 402 (1–2) (2014) 76–81, https://doi.org/10.1016/j.jim.2013.11.006.
[50] L.M. Varela, A. Ortega-Gomez, S. Lopez, R. Abia, F.J.G. Muriana, B. Bermudez, The effects of dietary fatty acids on the postprandial triglyceride-rich lipoprotein/apoB48 receptor axis in human monocyte/macrophage cells, J. Nutr. Biochem. 24 (12) (2013) 2031–2039, https://doi.org/10.1016/j.jnutbio.2013.07.004.
[51] I.J. Hidalgo, T.J. Raub, R.T. Borchardt, Characterization of the human colon carcinoma cell line (Caco-2) as a model system for intestinal epithelial permeability, Gastroenterology 96 (3) (1989) 736–749.
[52] I. Caro, X. Boulenc, M. Rousset, V. Meunier, M. Bourrié, B. Julian, H. Joyeux, C. Roques, Y. Berger, A. Zweibaum, G. Fabre, Characterisation of a newly isolated Caco-2 clone (TC-7), as a model of transport processes and biotransformation of drugs, Int. J. Pharm. 116 (2) (1995) 147–158, https://doi.org/10.1016/0378-5173(94)00280-I.
[53] P. Zeller, T. Bricks, G. Vidal, S. Jacques, P.M. Anton, E. Leclerc, Multiparametric temporal analysis of the Caco-2/TC7 demonstrated functional and differentiated monolayers as early as 14 days of culture, Eur. J. Pharm. Sci. 72 (2015) 1–11, https://doi.org/10.1016/j.ejps.2015.02.013.
[54] A.M. Barnett, N.C. Roy, W.C. McNabb, A.L. Cookson, Effect of a semi-purified oligosaccharide-enriched fraction from caprine Milk on barrier integrity and mucin production of co-culture models of the small and large intestinal epithelium, Nutrients 8 (5) (2016), https://doi.org/10.3390/nu8050267 article 5.
[55] I. Lozoya-Agullo, F. Araújo, I. González-Álvarez, M. Merino-Sanjuán, M. González-Álvarez, M. Bermejo, B. Sarmento, Usefulness of Caco-2/HT29-MTX and Caco-2/HT29-MTX/Raji B Coculture models to predict intestinal and colonic permeability compared to Caco-2 monoculture, Mol. Pharm. 14 (4) (2017) 1264–1270, https://doi.org/10.1021/acs.molpharmaceut.6b01165.
[56] N. Navabi, M.A. McGuckin, S.K. Lindén, Gastrointestinal cell lines form polarized epithelia with an adherent mucus layer when cultured in semi-wet interfaces with mechanical stimulation, PLoS One 8 (7) (2013) e68761, https://doi.org/10.1371/journal.pone.0068761.
[57] C. Hilgendorf, H. Spahn-Langguth, C.G. Regårdh, E. Lipka, G.L. Amidon, P. Langguth, Caco-2 versus Caco-2/HT29-MTX co-cultured cell lines : Permeabilities via diffusion, inside- and outside-directed carrier-mediated transport, J. Pharm. Sci. 89 (1) (2000) 63–75, https://doi.org/10.1002/(SICI)1520-6017(200001)89:1<63::AID-JPS7>3.0.CO;2-6.
[58] S.M. Moyes, J.F. Morris, K.E. Carr, Macrophages increase microparticle uptake by enterocyte-like Caco-2 cell monolayers, J. Anat. 217 (6) (2010) 740–754, https://doi.org/10.1111/j.1469-7580.2010.01304.x.
[59] H. Satsu, J.S. Hyun, H.S. Shin, M. Shimizu, Suppressive effect of an isoflavone fraction on tumor necrosis factor-alpha-induced interleukin-8 production in human intestinal epithelial Caco-2 cells, J. Nutr. Sci. Vitaminol. 55 (5) (2009) 442–446, https://doi.org/10.3177/jnsv.55.442.
[60] Lee, Intestinal permeability regulation by tight junction : implication on inflammatory bowel diseases, Intest. Res. 13 (1) (2015) 11–18, https://doi.org/10.5217/ir.2015.13.1.11.
[61] T. Suzuki, Regulation of intestinal epithelial permeability by tight junctions, Cell. Mol. Life Sci. 70 (4) (2013) 631–659, https://doi.org/10.1007/s00018-012-1070-x.
[62] M. Calatayud, J.V. Gimeno-Alcañiz, V. Devesa, D. Vélez, Proinflammatory effect of trivalent arsenical species in a co-culture of Caco-2 cells and peripheral blood mononuclear cells, Arch. Toxicol. 89 (4) (2015) 555–564, https://doi.org/10.1007/s00204-014-1271-1.
[63] N. Galińska, J. Topa, M. Tanska, A. Cieślińska, E. Fiedorowicz, H. Savelkoul, B. Jarmołowska, Modulatory effects of Osthole on lipopolysaccharides-induced inflammation in Caco-2 cell monolayer and co-cultures with THP-1 and THP-1-derived macrophages, Nutrients 13 (2020) 123, https://doi.org/10.3390/nu13010123.
[64] M.J. Haddad, J. Zuluaga-Arango, H. Mathieu, N. Barbezier, P.M. Anton, Intestinal epithelial co-culture sensitivity to pro-inflammatory stimuli and polyphenols is medium-independent, Int. J. Mol. Sci. 25 (13) (2024), https://doi.org/10.3390/ijms25137360. Article 13.
[65] Vamadevan, Arunan S., Masayuki Fukata, Elizabeth T. Arnold, Lisa S. Thomas, David Hsu, Maria T. Abreu. Regulation of Toll-like Receptor 4-Associated MD-2 in Intestinal Epithelial Cells: A Comprehensive Analysis. *Innate Immunity* 16 (2) (avril 2010): 93-103. 10.1177/1753425909339231.
[66] M. Cavicchi, B.J.R Whittle, Regulation of Induction of Nitric Oxide Synthase and the Inhibitory Actions of Dexamethasone in the Human Intestinal Epithelial Cell Line, Caco-2: Influence of Cell Differentiation, British J. Pharmacol. 128 (3) (1999) 705–715, https://doi.org/10.1038/sj.bjp.0702827.
[67] Kolios, George., Vassilis, Valatas., Stephen G. Ward. Nitric Oxide in Inflammatory Bowel Disease: A Universal Messenger in an Unsolved Puzzle. *Immunology*. 113 (4): 427-437.doi: 10.1111/j.1365-2567.2004.01984.x. (décembre 2004).
[68] Károly Palatka, Serfozo Zoltán, Veréb Zoltán, Hargitay Zoltán, Lontay Bea, Erdodi Ferenc, Bánfalvi Gáspár, Nemes Zoltán, Udvardy Miklós, Altorjay István, Changes in the Expression and Distribution of the Inducible and Endothelial Nitric Oxide Synthase in Mucosal Biopsy Specimens of Inflammatory Bowel Disease, Scandinavian Journal of Gastroenterology 40 (6) (2005) 670–680, https://doi.org/10.1080/00365520510015539.
[69] Mayura Somchit, Changtam Chatchawan, Kimseng Rungruedi, Utaipan Tanyarath, Lertcanawanichakul Monthon, Suksamrarn Apichart, Chunglok Warangkana, Demethoxycurcumin from Curcuma Longa Rhizome Suppresses iNOS Induction in an in Vitro Inflamed Human Intestinal Mucosa Model, Asian Pacific Journal of Cancer Prevention: APJCP 15 (4) (2014) 1807–1810, https://doi.org/10.7314/apjcp.2014.15.4.1807.
[70] F. Leonard, E.-M. Collnot, C.-M. Lehr, A three-dimensional Coculture of enterocytes, monocytes and dendritic cells to model inflamed intestinal mucosa in vitro, Mol. Pharm. 7 (6) (2010) 2103–2119, https://doi.org/10.1021/mp1000795.
[71] S. Prasad, R. Mingrino, K. Kaukinen, K.L. Hayes, R.M. Powell, T.T. MacDonald, J. E. Collins, Inflammatory processes have differential effects on claudins 2, 3 and 4 in colonic epithelial cells, Lab. Investig. 85 (9) (2005) 1139–1162, https://doi.org/10.1038/labinvest.3700316.
[72] N. Li, D. Wang, Z. Sui, X. Qi, L. Ji, X. Wang, L. Yang, Development of an improved three-dimensional in vitro intestinal mucosa model for drug absorption evaluation, Tissue Eng. Part C Methods 19 (9) (2013) 708–719, https://doi.org/10.1089/ten.TEC.2012.0463.
[73] C. Song, Z. Chai, S. Chen, H. Zhang, X. Zhang, Y. Zhou, Intestinal mucus components and secretion mechanisms : what we do and do not know, Exp. Mol. Med. 55 (4) (2023) 681–691, https://doi.org/10.1038/s12276-023-00960-y.
[74] J. Iwashita, Y. Sato, H. Sugaya, N. Takahashi, H. Sasaki, T. Abe, mRNA of MUC2 is stimulated by IL-4, IL-13 or TNF-α through a mitogen-activated protein kinase pathway in human colon cancer cells, Immunol. Cell Biol. 81 (4) (2003) 275–282, https://doi.org/10.1046/j.1440-1711.2003.t01-1-01163.x.
[75] M.G. Smirnova, S.L. Kiselev, J.P. Birchall, J.P. Pearson, Up-regulation of mucin secretion in HT29-MTX cells by the pro-inflammatory cytokines tumor necrosis factor-alpha and interleukin-6, Eur. Cytokine Netw. 12 (1) (2001) 119–125.
[76] M.A. McGuckin, R. Eri, L.A. Simms, T.H.J. Florin, G. Radford-Smith, Intestinal barrier dysfunction in inflammatory bowel diseases, Inflamm. Bowel Dis. 15 (1) (2009) 100–113, https://doi.org/10.1002/ibd.20539.
[77] W.A. Petri, C. Naylor, R. Haque, Environmental enteropathy and malnutrition : do we know enough to intervene? BMC Med. 12 (2014) https://doi.org/10.1186/s12916-014-0187-1.
[78] D. Hwang, M.-J. Kang, C.-W. Kang, G.-D. Kim, Kaempferol-3-O-β-rutinoside suppresses the inflammatory responses in lipopolysaccharide-stimulated RAW264.7 cells via the NF-κB and MAPK pathways, Int. J. Mol. Med. 44 (6) (2019) 2321–2328, https://doi.org/10.3892/ijmm.2019.4381.
[79] C. Tian, X. Liu, Y. Chang, R. Wang, M. Yang, M. Liu, Rutin prevents inflammation induced by lipopolysaccharide in RAW 264.7 cells via conquering the TLR4-MyD88-TRAF6-NF-κB signalling pathway, J. Pharm. Pharmacol. 73 (1) (2021) 110–117, https://doi.org/10.1093/jpp/rgaa015.
[80] J. Shan, J. Fu, Z. Zhao, X. Kong, H. Huang, L. Luo, Z. Yin, Chlorogenic acid inhibits lipopolysaccharide-induced cyclooxygenase-2 expression in RAW264.7 cells through suppressing NF-kappaB and JNK/AP-1 activation, Int. Immunopharmacol. 9 (9) (2009) 1042–1048, https://doi.org/10.1016/j.intimp.2009.04.011.
[81] S.-K. Bai, S.-J. Lee, H.-J. Na, K.-S. Ha, J.-A. Han, H. Lee, Y.-G. Kwon, C.-K. Chung, Y.-M. Kim, Beta-carotene inhibits inflammatory gene expression in lipopolysaccharide-stimulated macrophages by suppressing redox-based NF-kappaB activation, Exp. Mol. Med. 37 (4) (2005) 323–334, https://doi.org/10.1038/emm.2005.42.
[82] Q. Bian, T. Qin, Z. Ren, D. Wu, F. Shang, Lutein or zeaxanthin supplementation suppresses inflammatory responses in retinal pigment epithelial cells and macrophages, Adv. Exp. Med. Biol. 723 (2012) 43–50, https://doi.org/10.1007/978-1-4614-0631-0_7.
[83] I. Boukhers, F. Boudard, S. Morel, A. Servent, K. Portet, C. Guzman, M. Vitou, J. Kongolo, A. Michel, P. Poucheret, Nutrition, healthcare benefits and phytochemical properties of cassava (*Manihot esculenta*) leaves sourced from three countries (Reunion, Guinea, and Costa Rica), Foods (Basel, Switzerland) 11 (14) (2022) 2027, https://doi.org/10.3390/foods11142027.
[84] J. Zhen, T.S. Villani, Y. Guo, Y. Qi, K. Chin, M.-H. Pan, C.-T. Ho, J.E. Simon, Q. Wu, Phytochemistry, antioxidant capacity, total phenolic content and anti-inflammatory activity of *Hibiscus sabdariffa* leaves, Food Chem. 190 (2016) 673–680, https://doi.org/10.1016/j.foodchem.2015.06.006.
[85] T. Suzuki, H. Hara, Quercetin enhances intestinal barrier function through the assembly of zonula [corrected] occludens-2, occludin, and claudin-1 and the expression of claudin-4 in Caco-2 cells, J. Nutr. 139 (5) (2009) 965–974, https://doi.org/10.3945/jn.108.100867.
[86] T. Suzuki, S. Tanabe, H. Hara, Kaempferol enhances intestinal barrier function through the cytoskeletal association and expression of tight junction proteins in Caco-2 cells, J. Nutr. 141 (1) (2011) 87–94, https://doi.org/10.3945/jn.110.125633.
[87] P. Xu, S. Luo, J. Song, Z. Dai, D. Li, C. Wu, Effect of sodium alginate-based hydrogel loaded with lutein on gut microbiota and inflammatory response in DSS-induced colitis mice, Food Sci. Human Wellness 12 (6) (2023) 2428–2439, https://doi.org/10.1016/j.fshw.2023.03.010.
[88] H. Grar, W. Dib, H. Gourine, H. Negaoui, B.H.F. Taleb, A. Louaar, S. Ouldhocine, H. Kaddouri, O. Kheroua, D. Saidi, β-Carotene improves intestinal barrier function by modulating proinflammatory cytokines and improving antioxidant capacity in β-lactoglobulin-sensitized mice, J. Biol. Regul. Homeost. Agents 34 (5) (2020) 1689–1697, https://doi.org/10.23812/20-24-A.
[89] E. Reboul, Proteins involved in fat-soluble vitamin and carotenoid transport across the intestinal cells : new insights from the past decade, Prog. Lipid Res. 89 (2023) 101208, https://doi.org/10.1016/j.plipres.2022.101208.
[90] G. Mulokozi, E. Hedrén, U. Svanberg, In vitro accessibility and intake of β-carotene from cooked green leafy vegetables and their estimated contribution to vitamin a

requirements, Plant Foods Hum. Nutr. 59 (1) (2004), https://doi.org/10.1007/s11130-004-4305-7. Article 1.
[91] A. During, E.H. Harrison, Intestinal absorption and metabolism of carotenoids : insights from cell culture, Arch. Biochem. Biophys. 430 (1) (2004) 77–88, https://doi.org/10.1016/j.abb.2004.03.024.
[92] Claudine Manach, Scalbert Augustin, Morand Christine, Rémésy Christian, Polyphenols: Food Sources and Bioavailability, The Am. J. Clinic. Nut. 79 (5) (2004) 727–747, https://doi.org/10.1093/ajcn/79.5.727.
[93] C. Mascaraque, C. Aranda, B. Ocón, M.J. Monte, M.D. Suárez, A. Zarzuelo, J.J. G. Marín, O. Martínez-Augustin, F.S. de Medina, Rutin has intestinal antiinflammatory effects in the CD4+ CD62L+ T cell transfer model of colitis, Pharmacol. Res. 90 (2014) 48–57, https://doi.org/10.1016/j.phrs.2014.09.005.
[94] A. Sharma, N.V. Tirpude, M. Kumari, Y. Padwad, Rutin prevents inflammation-associated colon damage via inhibiting the p38/MAPKAPK2 and PI3K/Akt/GSK3β/NF-κB signalling axes and enhancing splenic Tregs in DSS-induced murine chronic colitis, Food Funct. 12 (18) (2021) 8492–8506, https://doi.org/10.1039/D1FO01557E.